ITUPublications

International Telecommunication Union
Radiocommunication Sector

Report ITU-R RS.2536-0

(09/2023)

RS Series: Remote sensing systems

Sharing and compatibility studies related to spaceborne radar sounders in the 40-50 MHz frequency band

Foreword

The role of the Radiocommunication Sector is to ensure the rational, equitable, efficient and economical use of the radio-frequency spectrum by all radiocommunication services, including satellite services, and carry out studies without limit of frequency range on the basis of which Recommendations are adopted.

The regulatory and policy functions of the Radiocommunication Sector are performed by World and Regional Radiocommunication Conferences and Radiocommunication Assemblies supported by Study Groups.

Policy on Intellectual Property Right (IPR)

ITU-R policy on IPR is described in the Common Patent Policy for ITU-T/ITU-R/ISO/IEC referenced in Resolution ITU-R 1. Forms to be used for the submission of patent statements and licensing declarations by patent holders are available from http://www.itu.int/ITU-R/go/patents/en where the Guidelines for Implementation of the Common Patent Policy for ITU-T/ITU-R/ISO/IEC and the ITU-R patent information database can also be found.

Series of ITU-R Reports

(Also available online at https://www.itu.int/publ/R-REP/en)

Series	Title
BO	Satellite delivery
BR	Recording for production, archival and play-out; film for television
BS	Broadcasting service (sound)
BT	Broadcasting service (television)
F	Fixed service
M	Mobile, radiodetermination, amateur and related satellite services
P	Radiowave propagation
RA	Radio astronomy
RS	**Remote sensing systems**
S	Fixed-satellite service
SA	Space applications and meteorology
SF	Frequency sharing and coordination between fixed-satellite and fixed service systems
SM	Spectrum management
TF	Time signals and frequency standards emissions

***Note**: This ITU-R Report was approved in English by the Study Group under the procedure detailed in Resolution ITU-R 1.*

Electronic Publication
Geneva, 2023

REPORT ITU-R RS.2536-0

Sharing and compatibility studies related to spaceborne radar sounders in the 40-50 MHz frequency band

(2023)

TABLE OF CONTENTS

Page

1 Introduction

This Report provides the results of a static and dynamic radio frequency interference (RFI) analysis for determining the degree of compatibility between a spaceborne very high frequency (VHF) 45 MHz centre frequency, 10 MHz bandwidth radar sounder, as described in Recommendation ITU-R RS.2042, and in-band, as well as selected out-of-band, incumbent services over the 40-50 MHz frequency band. It describes the analysis methodology and documents the results of a series of simulations that have been based upon actual system specifications and operational factors. Although the simulations in this document were carried out using a specific proposed system whose characteristics are known, it is expected that the results would also apply to other potential spaceborne radar sounders systems with similar characteristics.

The results presented in this Report are based on some assumptions and characteristics related to the affected services that were not fully agreed upon. Therefore, the presented results may not correspond to real operational conditions.

2 Radar sounder characteristics and operation

2.1 Mission objectives

The spaceborne active sensor operating in the 40-50 MHz range will produce sub-surface data with a vertical resolution of 5-7 m, and will have a surface signal-to-noise ratio (SNR) of approximately 66 dB. The mission's scientific objectives are:

1) to understand the global thickness, inner structure, and the thermal stability of the Earth's ice sheets (e.g. in Greenland and Antarctica) as an observable parameter of Earth climate evolution, and

2) to understand the occurrence, distribution, and dynamics of the earth fossil aquifers in desertic environments such as northern Africa and the Arabian Peninsula as key elements in understanding recent paleoclimatic changes.

2.2 Design parameters

A proposed system for the Earth orbiting sounding radar is an Earth enhanced duplicate of the Shallow Radar Sounder (SHARAD) which was a Mars orbiting sounding radar operating in the 15-25 MHz frequency range. The resulting radar data will be used in the study of the Earth's subsurface with radar mapping of subsurface scattering layers with the intent to locate water/ice deposits. The characteristics and orbital parameters of the proposed system are shown in Table 1.

TABLE 1

Spaceborne sounding radar characteristics in the 40-50 MHz range

Sensor characteristics	
Parameter	**Value**
Sensor type	Radar sounder
Orbit characteristics	
Type of orbit	Circular, SSO[1]
Altitude (km)	400
Inclination (degree)	97

1 Sun-Synchronous Orbit (SSO).

TABLE 1 *(end)*

Sensor characteristics	
Parameter	**Value**
Ascending node LST	004:00
Eccentricity	0
Orbits per day	15.8
Repeat period (days)	548
Antenna characteristics	
Antenna type	9 element cross Yagi
Number of beams	1
Antenna peak gain (transmit and receive) (dBi)	10
Polarization	Circular
Antenna beam look angle (degree)	Nadir
Antenna beam azimuth angle (degree)	Nadir
Antenna elevation −3 dB beamwidth (degree)	40
Antenna azimuth −3 dB beamwidth (degree)	40
Sensor antenna pattern	See Fig. 1
Transmitter characteristics	
RF centre frequency (MHz)	45
RF 3 dB bandwidth (MHz)	8
RF 20 dB bandwidth (MHz)	10
Transmit peak power (dBW)	20
Chirp bandwidth (MHz)	10
Pulse width (μs)	85
Pulse repetition frequency (PRF) (Hz)	1200
Pulse modulation	Linear FM (LFM) chirp (see Fig. 5)
Receiver characteristics	
RF centre frequency (MHz)	45
Gain (dB)	40-50
SNR (dB)	30
LNA bandwidth (MHz)	> 100
Final IF filter bandwidth (MHz)	12
System noise figure (dB)	5
Minimum detectable signal level (dBm)	−132
I/*N* (dB)	−6
Dynamic range (dB)	< 20
Emission characteristics	
Maximum mean pfd (dB (W/(m^2 · 4 kHz)))[2]	−135.96
Maximum peak pfd (dB (W/(m^2 · 4 kHz)))[3]	−126.05

2 Calculated via the formula given in **21.16.8** of the Radio Regulations (RR) Articles, Edition of 2020, which applies for clear sky conditions incorporating only free space path loss effects.

3 Computed as is done the average pfd, but with the terms due to the pulse duty cycle, namely the pulse repetition frequency (PRF) and the pulse width, removed.

The antenna gain pattern of the proposed system has a peak gain of 10 dBi, and a beamwidth of 40 degrees in range and azimuth. For the sharing studies presented in this Report, it was assumed that the antenna gain pattern was only a function of the off-boresight angle, with an antenna gain pattern as shown in Fig. 1.

FIGURE 1

9-element Yagi antenna pattern

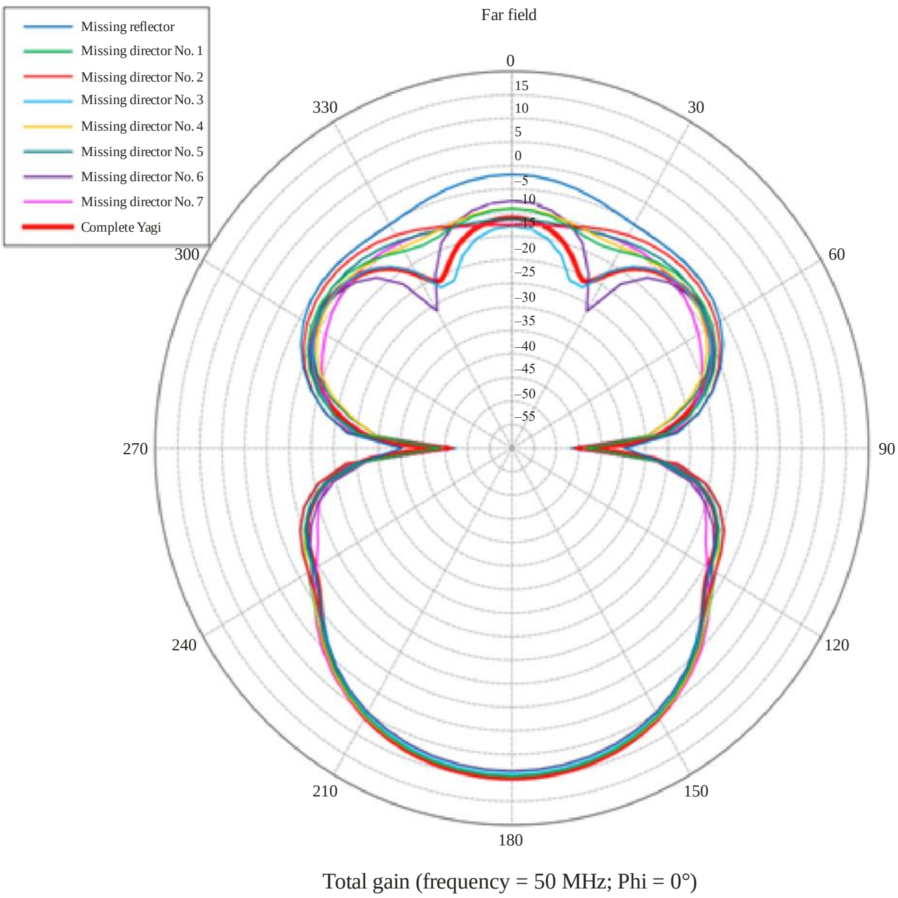

For the sharing studies presented in this Report, it was assumed that the antenna gain pattern was only a function of the off-boresight angle. Specifically, the antenna gain pattern used in the simulations presented in this report is as shown in Fig. 2.

FIGURE 2

Spaceborne VHF radar sounder antenna gain used in the sharing studies

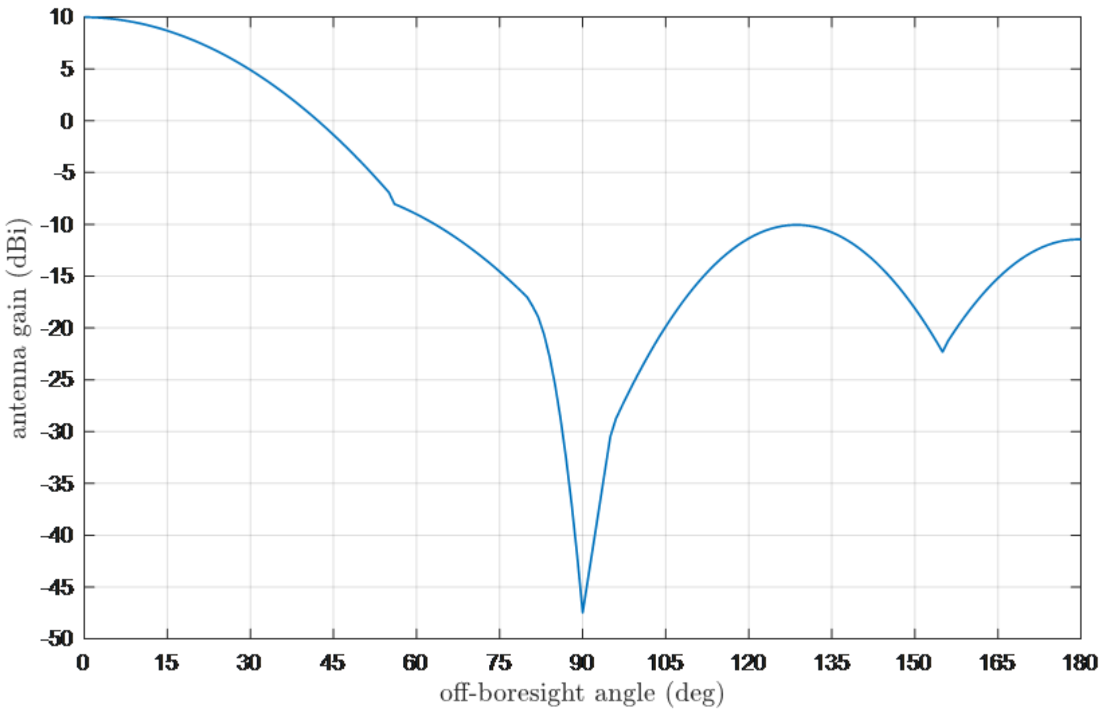

2.3 Orbital parameters

Spaceborne active sensors of this type are expected to be deployed on low-Earth orbiting satellites, at an inclination optimized for a Sun-synchronous orbit and with an eccentricity less than 0.001. Orbital parameters of the proposed system can be found in Table 1.

2.4 Operational limitations

Sounding radars in the 40-50 MHz range are designed to operate in un-inhabited or sparsely populated areas of the ice sheets (e.g. in Greenland and Antarctica) and the deserts (e.g. in northern Africa and the Arabian Peninsula) and for limited time intervals. For example, the operation of the proposed missions is expected not to exceed 10 minutes in duration per 92.7 minutes orbit.

Areas of coverage for the proposed regions of operations that depict the geographic area over which the transmitted signal will be propagated are included in Fig. 3.

FIGURE 3

Spaceborne radar sounder coverage

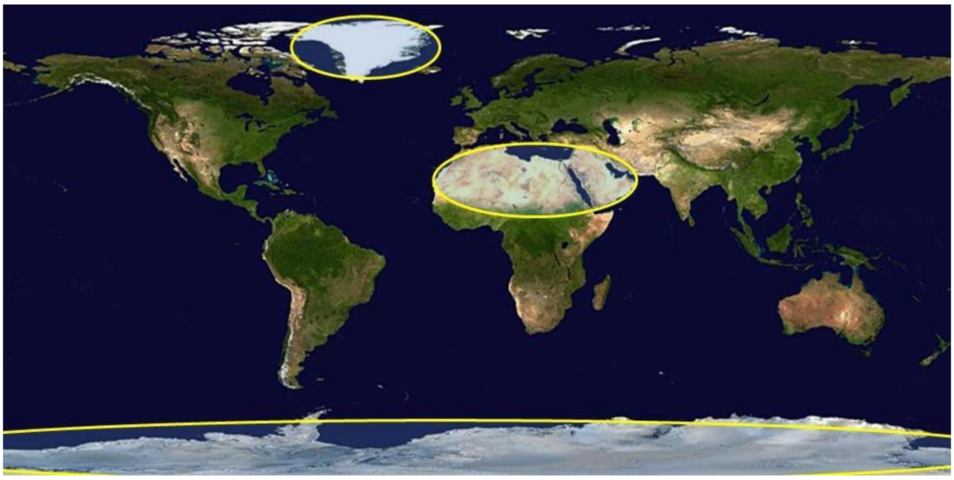

The sounding radars are designed to be operated only in a few hours window centred approximately around 4 a.m. local time, with respect to the location of the centre of the radar sensor footprint. These times were chosen because ionospheric perturbations to the radar signal are at a minimum during this time period and use of the spectrum by other services is expected to be the lightest.

It is also important to note that this study considers the operational scientific objectives and constraints of the radar sounder described in Recommendation ITU-R RS.2042. The study of this Report considers the impact of one operational sounder on incumbent services allocated in and around the 40-50 MHz frequency range. Taking into account the high investment cost associated with this type of sensor with observations in the 40-50 MHz band, the number of spaceborne radar sounder missions operating simultaneously is expected to remain very small; perhaps only one, or two, in number. The results presented in this study only consider interference from a single radar sounder and do not take into account aggregate interference effects from multiple sounders.

2.5 Footprint of radar sounder

Referring to Table 1, with an altitude of 400 km for the spaceborne radar sounder, along with an Earth nadir oriented transmit antenna with a 3 dB beamwidth of 40 degrees, the footprint of the spaceborne VHF radar sounder corresponds to a spherical cap along the surface of the Earth with a surface area of 67156.8 km^2. The radius of the base of this spherical cap is 146.2 km. A view of the spaceborne VHF radar sounder sensor footprint seen along the surface of the Earth is shown in Fig. 4, assuming a Cartesian view of the Earth. In this example, the location was chosen to lie within the Greenland area which is one of the intended areas of operation targeted for the radar sounder.

FIGURE 4

Radar sounder footprint along the surface of the Earth

2.6 Emission spectrum

Figure 5 shows the typical chirp emission spectrum for a radar sounder waveform operating in the frequency range of 40-50 MHz, as characterized in Table 1. In practice, bandpass filtering is often applied to attenuate the out-of-band power. For all simulations presented in this report, most notably those in Annex 1, § A1.5 and Annex 2 pertaining to interference to out-of-band services, the radar sounder under investigation has been assumed to have an emission spectrum as shown in Fig. 5. The results can be readily adjusted to reflect a different emission spectrum as needed.

FIGURE 5

Typical chirp emission spectrum

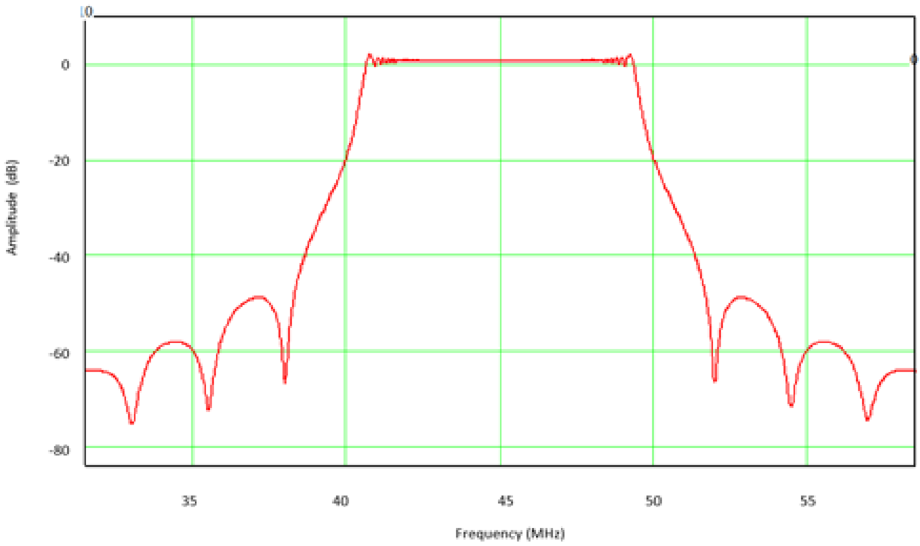

3 Overview of incumbent services operating within and in the vicinity of the 40-50 MHz frequency band

Allocations for incumbent services can be found in the Radio Regulations (RR) Articles, Edition of 2020, in Section IV – Table of Frequency Allocations. A list of the incumbent services operating around ±10 MHz of the 40-50 MHz frequency band occupied by the spaceborne VHF radar sounder can be found in Table 2. Specifically, the services allocated over the frequency range 30-68 MHz are indicated, and the classification of each service (i.e. primary or secondary) is specified according to the capitalization convention for the services (namely, primary services are in all capital letters, while secondary services only have the first letter capitalized).

TABLE 2

Description of incumbent services operating over the 30-68 MHz frequency range (i.e. around ±10 MHz of the 40-50 MHz frequency band occupied by the spaceborne VHF radar sounder), taken from the RR Articles, Edition of 2020, Section IV – Table of Frequency Allocations

<table>
<tr><th colspan="3">Allocation to services</th></tr>
<tr><th>Region 1 Table</th><th>Region 2 Table</th><th>Region 3 Table</th></tr>
<tr><td colspan="3">30.005-30.01 MHz
SPACE OPERATION (satellite identification)
FIXED
MOBILE
SPACE RESEARCH</td></tr>
<tr><td colspan="3">30.01-37.5 MHz
FIXED
MOBILE</td></tr>
<tr><td colspan="3">37.5-38.25 MHz
FIXED
MOBILE
Radio astronomy
5.149</td></tr>
<tr><td>38.25-39 MHz
FIXED
MOBILE</td><td rowspan="3">38.25-39.986 MHz
FIXED
MOBILE</td><td rowspan="2">38.25-39.5 MHz
FIXED
MOBILE</td></tr>
<tr><td>39-39.5 MHz
FIXED
MOBILE
Radiolocation 5.132A
5.159</td></tr>
<tr><td>39.5-39.986 MHz
FIXED
MOBILE</td><td>39.5-39.986 MHz
FIXED
MOBILE
RADIOLOCATION 5.132A</td></tr>
<tr><td colspan="2" rowspan="2">39.986-40.02 MHz
FIXED
MOBILE
Space research</td><td>39.986-40 MHz
FIXED
MOBILE
RADIOLOCATION 5.132A
Space research</td></tr>
<tr><td>40-40.02 MHz
FIXED
MOBILE
Space research</td></tr>
</table>

TABLE 2 *(end)*

<table>
<tr><th colspan="3">Allocation to services</th></tr>
<tr><th>Region 1 Table</th><th>Region 1 Table</th><th>Region 1 Table</th></tr>
<tr><td colspan="3">40.02-40.98 MHz
FIXED
MOBILE
5.150</td></tr>
<tr><td colspan="3">40.98-41.015 MHz
FIXED
MOBILE
Space research
5.160 5.161</td></tr>
<tr><td colspan="3">41.015-42 MHz
FIXED
MOBILE
5.160 5.161 5.161A</td></tr>
<tr><td colspan="2">42-42.5 MHz
FIXED
MOBILE
Radiolocation 5.132A
5.160 5.161B</td><td>42-42.5 MHz
FIXED
MOBILE
5.161</td></tr>
<tr><td colspan="3">42.5-44 MHz
FIXED
MOBILE
5.160 5.161 5.161A</td></tr>
<tr><td colspan="3">44-47 MHz
FIXED
MOBILE
5.162 5.162A</td></tr>
<tr><td>47-50 MHz
BROADCASTING
5.162A 5.163 5.164 5.165</td><td>47-50 MHz
FIXED
MOBILE</td><td>47-50 MHz
FIXED
MOBILE
BROADCASTING
5.162A</td></tr>
<tr><td>50-52 MHz
BROADCASTING
Amateur 5.166A 5.166B 5.166C 5.166D 5.166E 5.169 5.169A 5.169B
5.162A 5.164 5.165</td><td colspan="2" rowspan="2">50-54 MHz
AMATEUR
5.162A 5.167 5.167A 5.168 5.170</td></tr>
<tr><td rowspan="2">52-68 MHz
BROADCASTING
5.162A 5.163 5.164 5.165 5.169 5.169A 5.169B 5.171</td></tr>
<tr><td>54-68 MHz
BROADCASTING
Fixed
Mobile
5.172</td><td>54-68 MHz
FIXED
MOBILE
BROADCASTING
5.162A</td></tr>
</table>

The services over this frequency range will be affected the most by the spaceborne VHF radar sounder characterized in § 2, most notably those in-band (i.e. operating within the 40-50 MHz frequency range). An in-depth look at the incumbent services within and in the vicinity of the frequency band 40-50 MHz which are the focus of the sharing studies in this Report are given in Table 3. Specifically, the interference protection criterion (IPC) of each service, along with the channel bandwidth (BW) over the VHF band of interest, and relevant International Telecommunication Union (ITU) Radiocommunication Sector (ITU-R) Recommendations, are provided in Table 3. Here, each IPC is given in terms of the interference-to-noise power spectral density (PSD) ratio *I*/*N*, given in dB.

TABLE 3

Incumbent services operating in and adjacent to the 40-50 MHz frequency band

Service	**40-50 MHz in/out-of-band status, Service category (primary (P) or secondary (S))**	**Interference protection criterion (IPC) *I*/*N* threshold limit (dB)**	**Channel bandwidth (BW) (kHz)**	**Relevant ITU-R Recommandations/Reports**
Fixed	In-band, (P)	−6	16, 36(1)	Rec. ITU-R F.758-7
Mobile	In-band, (P)	−6, −10(2)	16, 25/75	Rec. ITU-R M.1808-1
Broadcasting	In-band, (P)	−20	96(3), 130/180(4), 7 000/8 000(4)	Rec. ITU-R BT.1895-0
Radiolocation	In-band, (S)	−6	125(5), 0.5/1.5(6), 200/ –2 200(7)	Report ITU-R M.2435-0, Rec. ITU-R M.1461, Rec. ITU-R M.1874-1, Rec. ITU-R M.1226
Space research	In-band, (S)	−6	1	Rec. ITU-R SA.1016-1, Rec. ITU-R SA.363-5
Amateur	Out-of-band, (P)	−6	1 072, 0.5, 2.7, 6, 9, 12, 16	Report ITU-R M.2478, Rec. ITU-R M.1732-2

(1) The channel BW values for the fixed service were provided by a liaison statement from ITU-R Working Party (WP) 5C. For a worst case scenario, the larger BW value of 36 kHz is used in the sharing studies.

(2) In Recommendation ITU-R M.1808-1, an *I*/*N* threshold value of −6 dB is nominally advocated, with the more stringent value of −10 dB reserved for applications with greater protection requirements, such as public protection and disaster relief (PPDR). In this report, both threshold values are considered in the sharing studies.

(3) The value of 96 kHz represents the channel bandwidth of the Digital Radio Mondiale (DRM) Mode E orthogonal frequency division multiplex (OFDM) system parameterized in Recommendation ITU-R BS.1114-12.

(4) Over the 47-68 MHz frequency range (Band I for the VHF broadcasting service), the Stockholm 1961 (ST61) agreement plan contains 377 sound broadcasting stations with bandwidths of 130 and 180 kHz, as well as 768 recorded analogue and television (TV) stations with bandwidths of 7 and 8 MHz.

(5) The channel BW value of 125 kHz was obtained from Report ITU-R M.2435-0. This value is used for the generic sharing studies with the radiolocation service.

(6) The channel BW values of 500 Hz and 1 500 Hz respectively correspond to the receiver intermediate frequency (IF) 3 dB BW for oceanographic radar Systems 4 and 9 described in Recommendation ITU-R M.1874-1. These values are used for sharing studies between the spaceborne VHF radar sounder and oceanographic radar (OR) systems operating over the frequency range 3-50 MHz.

(7) The channel BW value range 0.2-2.2 MHz corresponds to the necessary BW range stipulated for wind profiler radar (WPR) systems operating in band in the vicinity of 50 MHz as described in Recommendation ITU-R M.1226.

4 Study methodology

In this section, a description of the analytical methodology used for the sharing/compatibility studies between the spaceborne VHF radar sounder characterized in § 2 and the incumbent services identified in Table 3 is detailed. This primarily deals with the computation of the IPC quantity *I*/*N* stipulated in the ITU-R recommendations listed in Table 3, as well as the interference exceedance level (IEL) radio frequency interference (RFI) metric defined subsequently in § 4.1. Time series of this quantity over a suitable observation epoch can be used to determine whether or not compatibility holds for a given incumbent service.

4.1 Calculation of the observed *I/N* and the interference exceedance level

In a dynamic RFI simulation sharing study, it is worthwhile generating time series of the observed *I*/*N* and comparing these values with the IPC thresholds stipulated in Table 3. As the IPC threshold can vary from service to service, the RFI metric which will be the primary focus of the compatibility studies in this Report is the interference exceedance level (IEL) defined below.

$$IEL \triangleq (I/N)_{\mathrm{obs}} - (I/N)_{\mathrm{IPC}} \tag{1}$$

where:

IEL : interference exceedance level (dB)

$(I/N)_{\mathrm{obs}}$: observed interference-to-noise power spectral density (PSD) ratio (dB)

$(I/N)_{\mathrm{IPC}}$: interference-to-noise PSD ratio interference protection criterion (IPC) limit for the particular incumbent service (dB).

In this setting, an IEL value less than 0 dB implies compliance with the respective recommended ITU-R limit for interference.

The observed interference-to-noise PSD ratio $(I/N)_{\mathrm{obs}}$ is calculated via the following equation:

$$(I/N)_{\mathrm{obs}} = I - N = P_r - 10\log(B_r) - 30 - N \tag{2}$$

where:

I : observed interference PSD (dBW/Hz)

P_r : received interference power over the victim bandwidth (dBW)

B_r : victim receiver 3 dB bandwidth for the particular incumbent service (kHz)

N : observed noise PSD (dBW/Hz).

Equations (1) and (2) hold for any type of interference power level (i.e. peak or mean).

4.1.1 Computation of the received interference power

Following the procedures set forth in Recommendation ITU-R M.1461, the interference power P_r from equation (2) can be calculated as follows:

1. Peak interference power: P_r

$$P_r = P_{TX} + G_{TX} + G_{RX} - L_{TX} - L_P - L_{RX} - FDR_{IF} \tag{3}$$

or

2. Mean interference power: P_{r_mean}

$$P_{r\_mean} = P_{TX} + 10\log(PRF) + 10\log(\tau) + G_{TX} + G_{RX} - L_{TX} - L_P - L_{RX} - FDR_{IF} \tag{4}$$

where:

P_r : peak received interference power (dBW)

P_{r_mean} : mean received interference power (dBW)
P_{TX} : peak transmitter output power (dBW)
G_{TX} : transmitter antenna gain (dBi)
G_{RX} : receiver antenna gain (dBi)
PRF : pulse repetition frequency (Hz)
τ : pulsewidth (s)
L_{TX} : transmit feeder and associated losses (feeder, connectors, etc.) (dB)
L_P : propagation path loss between transmitting and receiving antennas (dB)
L_{RX} : receiver feeder and associated losses (feeder, connectors, etc.) (dB)
FDR_{IF} : frequency dependent rejection (FDR) produced by the receiver IF selectivity curve on an unwanted transmitter emission spectra (dB).

Equations (3) and (4) have been used in the simulations presented in this Report.

Equation (3) is the basis for interference calculations for the spaceborne radar sounder at peak power. Taking into account that RR No. **21.16.8** proposes for EESS (active) the use of mean pfd values, equation (4) establishes the calculation of the mean interference power P_r.

Receiver antenna gain (when no specific information was available)

For many of the incumbent service systems expected to be impacted by the spaceborne VHF radar sounder, a receiver antenna gain pattern was not available. This may be due to the fact that for lower frequency ranges, such as the 40-50 MHz VHF band under consideration, directionality of the antenna gain requires a larger aperture than for higher frequency bands. To account for some directionality of receiver antenna gain in the sharing studies, for all such studies for which there is no receiver antenna gain pattern provided, a half-wave dipole antenna gain pattern was assumed. This antenna gain pattern is a function of the off-axis angle α from the dipole, as illustrated in Fig. 6.

FIGURE 6

Illustration of half-wave dipole with off-axis angle

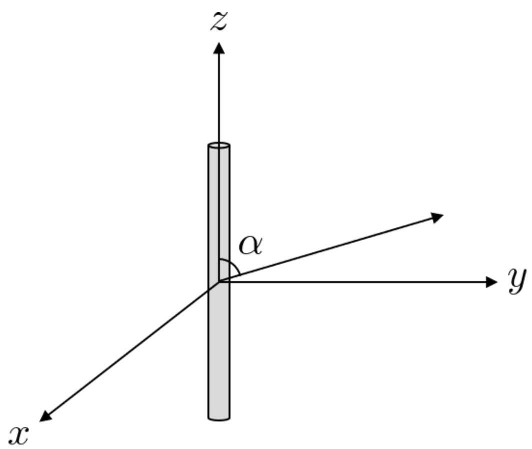

A closed form expression for the antenna gain of a half-wave dipole as a function of the off-axis angle α is shown below in equation (5).

$$G_{RX}(\alpha) = 2.15 + 20\log\left[\frac{\cos\left(\frac{\pi}{2}\cos\left(\frac{\pi}{180°}\alpha\right)\right)}{\sin\left(\frac{\pi}{180°}\alpha\right)}\right] \quad (5)$$

where:

G_{RX} : receiver antenna gain (dBi)

α : off-axis angle from half-wave dipole (degree).

A plot of the gain pattern of a half-wave dipole as a function of the off-axis angle α is shown in Fig. 7. From this Figure, it can be seen that the gain peaks at a value of 2.15 dBi, when the off-axis angle is 90 degrees.

FIGURE 7

Half-wave dipole antenna gain pattern as a function of off-axis angle

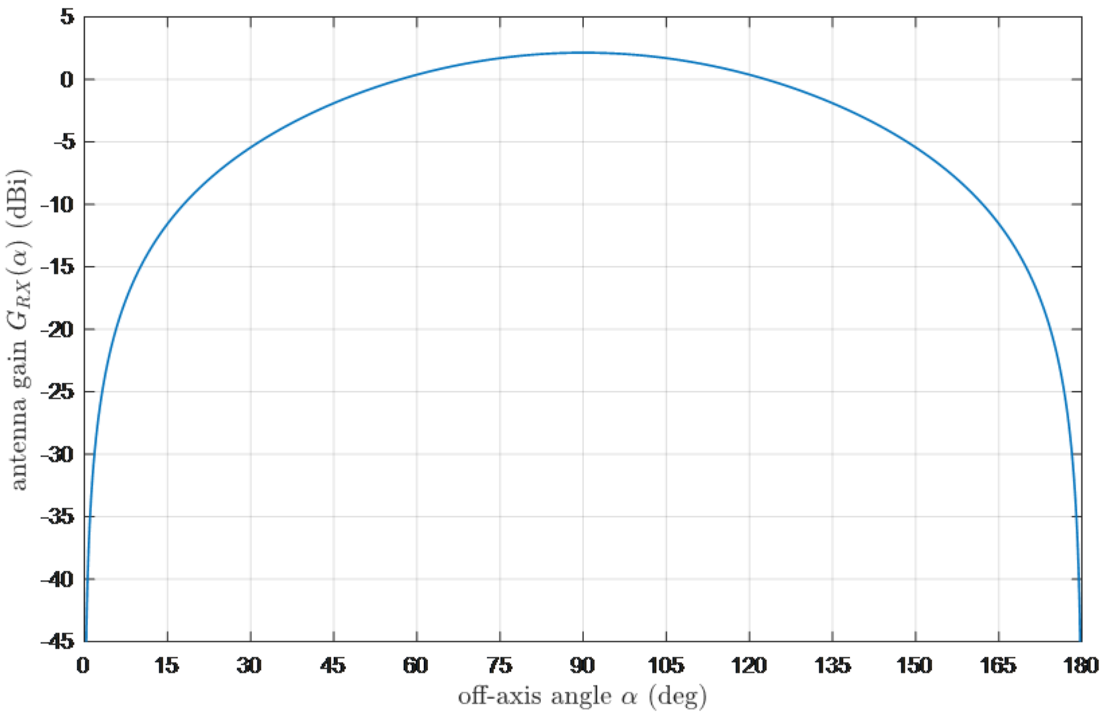

As most of the incumbent service systems are terrestrial, nominally, it will be assumed that the half-wave dipole is oriented at Earth zenith, with a possible tilt or pointing angle β, which will typically be small as the directive gain will usually be towards the horizon.

Propagation loss

Here, the propagation path loss factor L_P from equation (3) and equation (4) is a combination of free space, polarization mismatch, and miscellaneous loss effects given by the following equation:

$$L_P = FSPL + L_{P,\text{pol}} + L_{P,\text{misc}} \quad (6)$$

where:

L_P : propagation path loss (dB)

$FSPL$: free space path loss (FSPL) (dB)

$L_{P,\text{pol}}$: polarization mismatch loss (dB)

$L_{P,\text{misc}}$: miscellaneous propagation path loss factor, which can include atmospheric effects and other losses (dB).

From Recommendation ITU-R P.525-4, the free space path loss (FSPL) from equation (6) is calculated as follows:

$$FSPL = 32.45 + 20\log(f) + 20\log(d) \quad (7)$$

where:

$FSPL$: free space path loss (FSPL) (dB)

f : frequency (MHz)

d : distance (km).

For example, using equation (7) with an operational frequency of 45 MHz at an orbital altitude of 400 km yields an FSPL of 117.55 dB.

At the VHF bands under consideration for this sharing study, propagation losses due to atmospheric effects can be predominantly attributed to ionospheric absorption effects, which are described in Recommendation ITU-R P.531. These are a function of the latitude at which the propagation occurs. Specifically, propagation losses in the polar regions, occurring at geomagnetic latitudes greater than 64° and at heights greater than about 30 km, which are due to auroral and/or polar cap effects, can be larger than those at mid-latitude regions.

For these regions, polar cap absorption events can last up to a few days possibly 10 to 12 times a year, during the peak of the sunspot cycle, with a great reduction in absorption during hours of darkness. In addition, for such regions, auroral absorption can also occur, which is often localized and with variations in periods on the order of minutes. In contrast, ionospheric absorption which occurs at mid-latitude geomagnetic values is notably lower than in the polar regions.

Frequency dependent rejection (FDR)

Returning to equations (3) and (4), according to Recommendations ITU-R M.1461 and Recommendation ITU-R RS.1260-2, the frequency dependent rejection (FDR) factor FDR_{IF} from equations (3) and (4) is a combination of on-tune rejection (OTR) and off-frequency rejection (OFR), which itself is a function of the frequency difference Δf between the interferer transmitter and the victim receiver. From equation (7) of Recommendation ITU-R M.1461:

$$FDR_{IF}(\Delta f) = OTR + OFR(\Delta f) \qquad (8)$$

where:

$FDR_{IF}(\Delta f)$: frequency dependent rejection (FDR) as a function of the frequency difference between the interferer transmitter and victim receiver Δf (dB)

OTR : on-tune rejection (OTR) (dB)

$OFR(\Delta f)$: off-frequency rejection (OFR) as a function of the frequency difference between the interferer transmitter and victim receiver Δf (dB).

For the sharing studies carried out in this report, the OFR from equation (8) was not factored in, and a value of 0 dB was used throughout.

The OTR from equation (8) is given as follows:

1. When using the Peak interference power from equation (3):

For chirped pulsed signals, the OTR factor is given by equations (10) and (11) from Recommendation ITU-R M.1461 and equations (4a) and (4b) in Recommendation ITU-R RS.1260-2, which is applicable to an input waveform with a chirped pulse type of frequency modulation.

$$OTR = \max(10\log(B_c/(B_{t\text{ in }r}^2\tau)) + 60, 0) \qquad (9)$$

where:

OTR : on-tune rejection (OTR) (dB)

B_c : transmitter emission chirp bandwidth (MHz)

$B_{t\text{ in }r}$: 3 dB bandwidth of transmitter emission appearing in receiver filter bandwidth, or the interfered receiver 3 dB bandwidth (kHz)

τ : transmitter emission chirped pulse width (μs).

Equation (9) was used, in combination with the peak interference power, for the sharing the compatibility studies presented in this Report in between the radar sounder and other radar systems.

2. When using the mean interference power from equation (4):

$$OTR = 10\log(B_t/B_r) \quad (10)$$

where:

OTR : on-tune rejection (OTR) (dB)

B_t : transmitter 3 dB bandwidth (Hz)

B_r : receiver 3 dB bandwidth (Hz).

Equation (10) was used, in combination with the mean interference power, for the sharing the compatibility studies presented in this report in between the radar sounder and other non-radar systems.

4.1.2 Computation of the received noise power spectral density

The noise PSD N from equation (2) is assumed to come from a combination of internal and external noise sources. Here, the internal noise is considered to be the result of the victim receiver implementation, whereas the external noise is taken to come from the outside environment between the interferer and victim. Assuming the internal and external noise sources are statistically independent, the overall noise PSD N can be calculated as follows:

$$N = 10\log\left(10^{(N_{\text{int}}/10)} + 10^{(N_{\text{ext}}/10)}\right) \quad (11)$$

where:

N : overall noise PSD including internal and external contributions (dBW/Hz)

N_{int} : internal noise PSD (dBW/Hz)

N_{ext} : external noise PSD (dBW/Hz).

In the event that the internal noise PSD N_{int} from equation (11) is not known, the overall noise PSD N is simply set to $N = N_{\text{ext}}$, which is the value given in equation (11) in the limit as $N_{\text{int}} \to -\infty$ dBW/Hz.

Internal noise PSD

Noise effects due to internal victim receiver system implementations are typically characterized either in terms of the noise figure (NF) or system noise temperature T_{sys}. In either case, the internal noise PSD N_{int} is calculated using the following equation:

$$N_{\text{int}} = 10\log(k_B T_0) + NF = 10\log(k_B T_{\text{sys}}) \approx -203.98 + NF \approx -228.60 + 10\log(T_{\text{sys}}) \quad (12)$$

$$N_{\text{int}} = 10\log(k_B T_{\text{sys}}) = 10\log(k_B T_0) + 10\log\left(10^{\frac{NF}{10}} - 1\right) \approx -203.98 + 10\log\left(10^{\frac{NF}{10}} - 1\right) \quad (13)$$

where:

N_{int} : internal noise PSD (dBW/Hz)

k_B : the Boltzmann constant $1.38064852 \times 10^{-23}$ J/K (J/K)

T_0 : standard noise temperature of 290 K (K)

NF : noise figure of victim receiver given by $NF = 10\log\left(\frac{T_{\text{sys}}}{T_0} + 1\right)$ (dB)

T_{sys} : system noise temperature (K).

As mentioned earlier, if no data is available regarding the victim receiver system, the internal noise PSD N_{int} is not taken into account, and the overall noise PSD N is simply set to $N = N_{\text{ext}}$, which is effectively the value given in equation (11) in the limit as $N_{\text{int}} \to -\infty$ dBW/Hz.

External noise PSD

Effects due to external radio noise sources are described at length in Recommendation ITU-R P.372. In particular, the external noise is modelled as a combination of three components: man-made noise, galactic noise, and atmospheric noise. Man-made noise depends on the frequency and the environment, galactic noise only depends on frequency, and atmospheric noise depends on frequency, time of day, and season. Assuming that each noise component is statistically independent from the others, the external noise PSD N_{ext} from equation (11) is given by the following equation:

$$N_{\text{ext}} = 10\log\left(10^{(N_{\text{man}}/10)} + 10^{(N_{\text{gal}}/10)} + 10^{(N_{\text{atm}}/10)}\right) \quad (14)$$

where:

N_{ext} : external noise PSD (dBW/Hz)

N_{man} : man-made noise PSD (dBW/Hz)

N_{gal} : galactic noise PSD (dBW/Hz)

N_{atm} : atmospheric noise PSD (dBW/Hz).

In Recommendation ITU-R P.372, each noise component PSD, denoted here as N_{comp}, is characterized in terms of a nominal noise figure F_a or median noise figure F_{am}, denoted here generically as F_{gen}. Similar to equation (12), the noise component PSD N_{comp} is given as follows:

$$N_{\text{comp}} = 10\log(k_B T_0) + F_{\text{gen}} \approx -203.98 + F_{\text{gen}} \quad (15)$$

where:

N_{comp} : noise component PSD (dBW/Hz)

k_B : the Boltzmann constant $1.38064852 \times 10^{-23}$ J/K (J/K)

T_0 : standard noise temperature of 290 K (K)

F_{gen} : generic noise figure (i.e. either the nominal F_a or median F_{am} noise figure) (dB).

As stated earlier, the man-made, galactic, and atmospheric noise components in equation (14) depend on several factors, most notably frequency. A plot of the dependency of the nominal noise figures of these components as a function of frequency can be found in Fig. 2 of Recommendation ITU-R P.372, which is reproduced below in Fig. 8.

FIGURE 8

Noise figure F_a and noise temperature T_a as a function of frequency for atmospheric, man-made, and galactic noise sources (reproduction of Fig. 2 in Rec. ITU-R P.372)

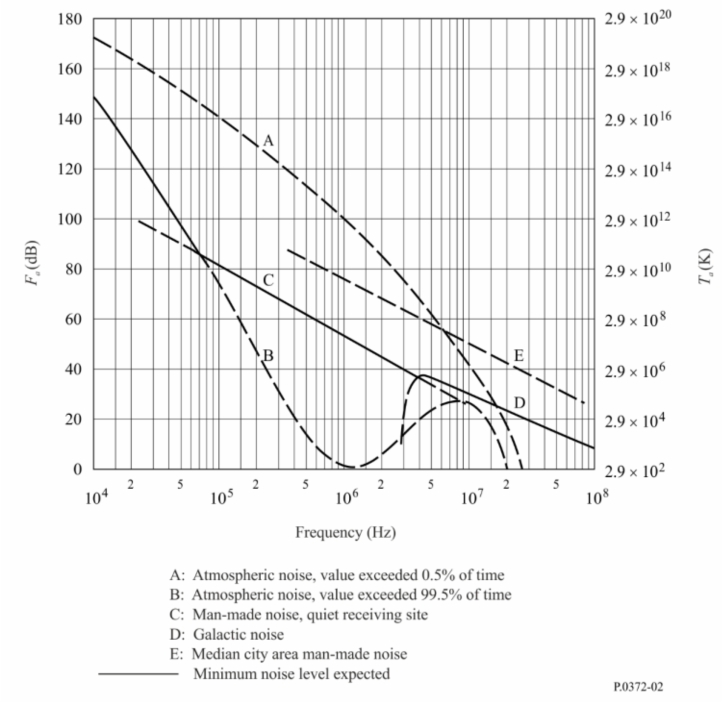

At the VHF frequency over which the spaceborne radar sounder is intended to operate, namely around 45 MHz, from Fig. 8, it can be seen that the noise factor for the atmospheric noise is below 0 dB, for both the cases in which the value is exceeded 0.5% and 99.5% of the time. As such, noise attributed to atmospheric effects is assumed negligible here for this study, and so the term in equation (14) due to N_{atm} was dropped, effectively meaning that the limit as $N_{\text{atm}} \to -\infty$ dBW/Hz was taken in this case.

From Recommendation ITU-R P.372, over the frequency range of interest, the median noise figures for the man-made and galactic noise components have been shown to approximately vary linearly with the logarithm of the frequency. This can be seen in Fig. 39 of Recommendation ITU-R P.372, which is reproduced here in Fig. 9. Specifically, the median noise figure F_{am} varies with the frequency f, according to the following model, as given in equation (15) of Recommendation ITU-R P.372, as reproduced below.

$$F_{am} = c - d \log f \tag{16}$$

where:

F_{am} : median noise figure (dB)

c, d : constants characterizing the median noise figure dependency with frequency

f : frequency (MHz).

FIGURE 9

Man-made and galactic median noise figure F_{am} as a function of frequency f over the band 0.3-250 MHz (Reproduction of Fig. 39 in Rec. ITU-R P.372)

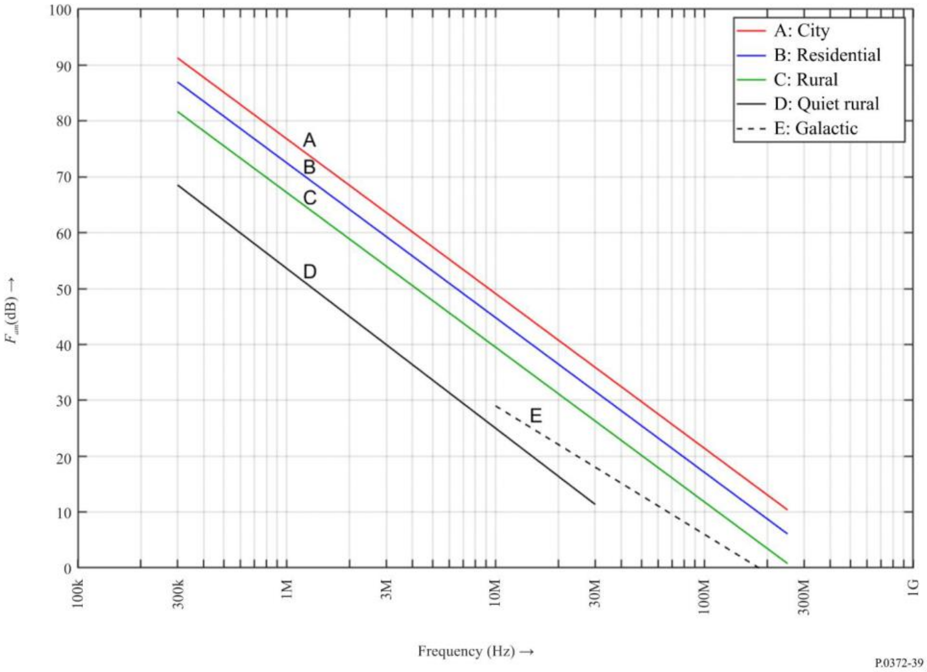

Values for the constants c and d from equation (16) are provided in Table 1 of Recommendation ITU-R P.372 and are reproduced here in Table 4. From Fig. 9, as only curves A, B, C and E are valid in the vicinity of the 45 MHz centre frequency of the spaceborne VHF radar sounder, only these curves have been used in the sharing studies contained in this Report.

TABLE 4

Values of the constants c and d in equation (16)
(Reproduction of Table 1 in Rec. ITU-R P.372)

Environmental category	c	d
City (curve A)	76.8	27.7
Residential (curve B)	72.5	27.7
Rural (curve C)	67.2	27.7
Quiet rural (curve D)	53.6	28.6
Galactic noise (curve E)	52.0	23.0

Using the values of c and d from Table 4 in equation (16), at the spaceborne VHF radar sounder frequency of $f = 45$ MHz, is obtained the median noise figure and noise component PSD values (see equation (15)) listed in Table 5.

TABLE 5

Median noise figure F_{am} and noise component PSD N_{comp} values at the spaceborne VHF radar sounder frequency of 45 MHz

Environmental category	Median noise figure F_{am} (dB)	Noise component PSD N_{comp} (dBW/Hz)
Man-made (city)	31.0	−172.97
Man-made (residential)	26.7	−177.27
Man-made (rural)	21.4	−182.57
Galactic	14.0	−190.00

Incorporating the man-made and galactic noise component PSD values from Table 5 in equation (14), it follows that the external noise PSD values for the city, residential, and rural environments are as shown in Table 6. These values were used in the sharing studies contained in this Report.

TABLE 6

External noise PSD N_{ext} values for a city, residential, and rural type of environment at the spaceborne VHF radar sounder frequency of 45 MHz

Environmental category	External noise PSD N_{ext} (dBW/Hz)
City	−172.88
Residential	−177.04
Rural	−181.85

Using the external noise PSD values given in Table 6, in tandem with the noise figure for a given victim receiver, one can calculate the overall noise PSD N from equation (11). From this, along with the victim receiver bandwidth, one can compute the received noise power P_n given below as follows:

$$P_n = N + 10\log(B_r) + 60 \quad (17)$$

where:

P_n : total received noise power over the victim bandwidth (dBm)

N : observed noise PSD (dBW/Hz)

B_r : victim receiver 3 dB bandwidth for the particular incumbent service (kHz).

The corresponding total received noise power for each of the external noise environments for the incumbent victim receiver systems considered throughout this study are given in Table 7.

TABLE 7

Total received noise power for the incumbent service systems considered in this study (parameterized according to external noise environment)

Victim system type	Total received noise power P_n (dBm)
FIXED	−97.32 (city) −101.48 (residential) −106.28 (rural)
MOBILE	−94.13 (city) −98.27 (residential) −103.04 (rural)
BROADCASTING (DRM)	−93.06 (city) −97.22 (residential) −102.02 (rural)
BROADCASTING (ST61 TV)	−73.85 (city) −78.01 (residential) −82.82 (rural)
Radiolocation	−91.91 (city) −96.07 (residential) −100.88 (rural)
Oceanographic radar (System 4)	−115.84 (city) −119.93 (residential) −124.48 (rural)
Oceanographic radar (System 9)	−111.11 (city) −115.24 (residential) −119.95 (rural)
Wind profiler radar	−79.46 (city) −83.62 (residential) −88.42 (rural)
Space research	−112.88 (city) −117.04 (residential) −121.85 (rural)
AMATEUR	−100.84 (city) −105.00 (residential) −109.80 (rural)

From the received noise power P_n given in equation (17), the observed interference-to-noise PSD ratio $(I/N)_{\text{obs}}$ is then given by the following:

$$(I/N)_{\text{obs}} = I - N = P_r - P_n \tag{18}$$

where:

$(I/N)_{\text{obs}}$: observed interference-to-noise PSD ratio (dB)

P_r : received interference power over the victim bandwidth (dBm)

P_n : total received noise power over the victim bandwidth (dBm).

Using equation (18), the received interference power P_r can be obtained from the observed interference-to-noise PSD $(I/N)_{\text{obs}}$ and the total received noise power P_n.

5 Set-up for sharing studies

Recall from Fig. 3 that the planned coverage areas for the spaceborne VHF radar sounder consist of sparsely populated areas of the ice sheets of Greenland and Antarctica and the deserts of northern Africa and the Arabian Peninsula. Therefore, different victim locations were selected, as follows:

a) Set-up for the studies in Annex 1

Setup for dynamic RFI simulations (general case)

The city of Ghardaïa in Algeria (a mid-latitude victim location) was selected as the victim location for this analysis. This site has the following location:

– Ghardaïa:
  - Latitude: 32°29′N,
  - Longitude: 3°40′E,
  - Altitude: 572 m.

In addition, to assess the impact of operations in Greenland upon areas in Canada, a victim location at the northernmost continuously inhabited place in the world, at Alert, in the Qikiqtaaluk Region of Nunavut, was also considered. This site has the following location:

– Alert:
  - Latitude: 82°30′N,
  - Longitude: 62°21′W,
  - Altitude: 68.1 m.

With this setup, a set of dynamic RFI simulations were carried out, in which the spaceborne VHF radar sounder described in Table 1, with a transmit antenna gain pattern as in Fig. 1, was considered. Specifically, the orbit of such a sounder was simulated and time series of the IEL from equation (1) were calculated for each simulation scenario.

Furthermore, the sounder was assumed to transmit according to the upper bound of its operational duty cycle (emission to operate for a period not to exceed 10 minutes in duration per 92.7 minute orbit) of $D_{op} = 10/92.7 \approx 0.1079$.

In the studies, the operational duty cycle is interpreted as a hardware limitation on emissions. In the dynamic simulations, a continuous 10-minute emission was assumed within each 92.7 minute window.

The geographical footprint corresponding to this 10 minute emission window is distributed across the world, depending upon the satellite orbit characteristics. It is not tied to any specific victim receiver location.

Annex 4 provides a sensitivity analysis, using a different value of operational duty cycle.

The intended usage of a window around 4.00 a.m. was not taken into account in those studies.

In order to represent a typical operational scenario for the sounder, each dynamic simulation was carried out over an 18-month period, with the relevant RFI metrics being calculated at 5-second increments. The specific observation epoch start/stop times considered for this set of analyses were as follows:

– Observation epoch start time: 2025/04/01 00:00:00 UTC,

– Observation epoch stop time: 2026/10/01 00:00:00 UTC,
– Observation epoch delta time (time increment): 5 s.
– Observation epoch number of data points: 9,469,440

Setup for dynamic RFI simulations only for the oceanographic radars

To reflect a potential realistic RFI scenario occurring from the use of a spaceborne VHF sounder over a coastal region in northern Africa, the oceanographic radar Systems 4 and 9 were assumed to be located in Tripoli, Libya. This site has the following location:

– Tripoli:
  - Latitude: 32°53’14”N,
  - Longitude: 13°11’29”E,
  - Altitude: 81 m.

For the purposes of the simulation, the oceanographic radars were oriented to point northward along the horizon, in the direction of the Mediterranean Sea. The orbit of the spaceborne VHF radar sounder was simulated over the same 18 month observation epoch.

Setup for dynamic RFI simulations only for wind profile radars

While Recommendation ITU-R M.1226 describes several parameters needed to simulate and characterize the RFI upon a WPR operating near 50 MHz, it does not offer a specific set of locations or beam direction orientations for WPR systems expected to be encountered. For this case study, the location and beam directions were derived from the following article in the literature:

– F. Saïd, et al., “Offshore winds obtained from a network of wind-profiler radars during HyMeX,” Quarterly Journal of the Royal Meteorological Society, Volume 142, Issue S1, pp. 23-42, August 2016.

In this article, several WPR systems operating at a centre frequency of 45 MHz are considered. The WPR closest to the expected operational zone of a spaceborne VHF radar sounder over northern Africa was selected as the location for this case study. From the article above, this was a 45 MHz WPR located in Pianottoli, on the island of Corsica. This site has the following location:

– Pianottoli:
  - Latitude: 41°28′N,
  - Longitude: 9°03′E,
  - Altitude: 21 m.

The above article also lists a set of beam directions used in the analysis contained therein. Several of these beam directions values (azimuth, off-zenith elevation) (°) were considered in this case study, including the following:

(0, 0), (340, 15), (30, 36), (300, 41).

For the dynamic RFI simulations considered for this case study, the orbit of the spaceborne VHF radar sounder was simulated over the same 18-month observation epoch and 5 s time increment. As no system noise temperature or noise figure value was specified for a representative WPR system operating near 50 MHz from Recommendation ITU-R M.1226, only an external noise source was considered for this analysis.

Additional calculations were also performed considering a specific WPR location at 68.57°S and 77.97°E (Davis, Antarctica).

b) Set-up for the studies in Annex 2

Two victim locations were considered:

1. A mid-latitude location: Ghardaïa for the studies related to FS, MS, BS, SRS and Amateur service:
   - Latitude: 32°29′N,
   - Longitude: 3°40′E,
   - Altitude: 572 m.
2. South Greenland for the studies related to Oceanographic radars and WPR:
   - Latitude: 66°50′N,
   - Longitude: 46°44′E,
   - Altitude: 10 m.

With this setup, also a set of dynamic RFI simulations were carried out, in which the spaceborne VHF radar sounder was considered. Each dynamic simulation was carried out over a 60-day period, with the relevant RFI metrics being calculated at 1 s increments. The specific observation epoch start/stop times considered for this set of analyses were as follows:

Observation epoch start time: 2025/04/01 00:00:00 UTC,

Observation epoch stop time: 2025/05/30 00:00:00 UTC,

Observation epoch delta time (time increment): 1 s.

An analysis of the temporal interference from EESS (active) into the mobile service was also performed, with a station located at Vilnius:

- Latitude: 56.23270°N,
- Longitude: 25.49110°E,
- Altitude: 10 m.

Additional calculations were also performed considering a specific WPR location at 68.57°S and 77.97°E (Davis, Antarctica).

c) Additional consideration on the set-up for studies in Annexes 1 and 2

An Earth Cartesian view of the dynamic simulation at the start of the observation epoch is shown in Fig. 10. In addition to showing the VHF sounder interferer and victim site locations at Ghardaïa and Alert, the orbit of the Sun-synchronous spaceborne sounder and 40° sensor footprint are also shown.

FIGURE 10

Earth Cartesian view of the dynamic spaceborne VHF radar sounder RFI simulation at the start of the observation epoch

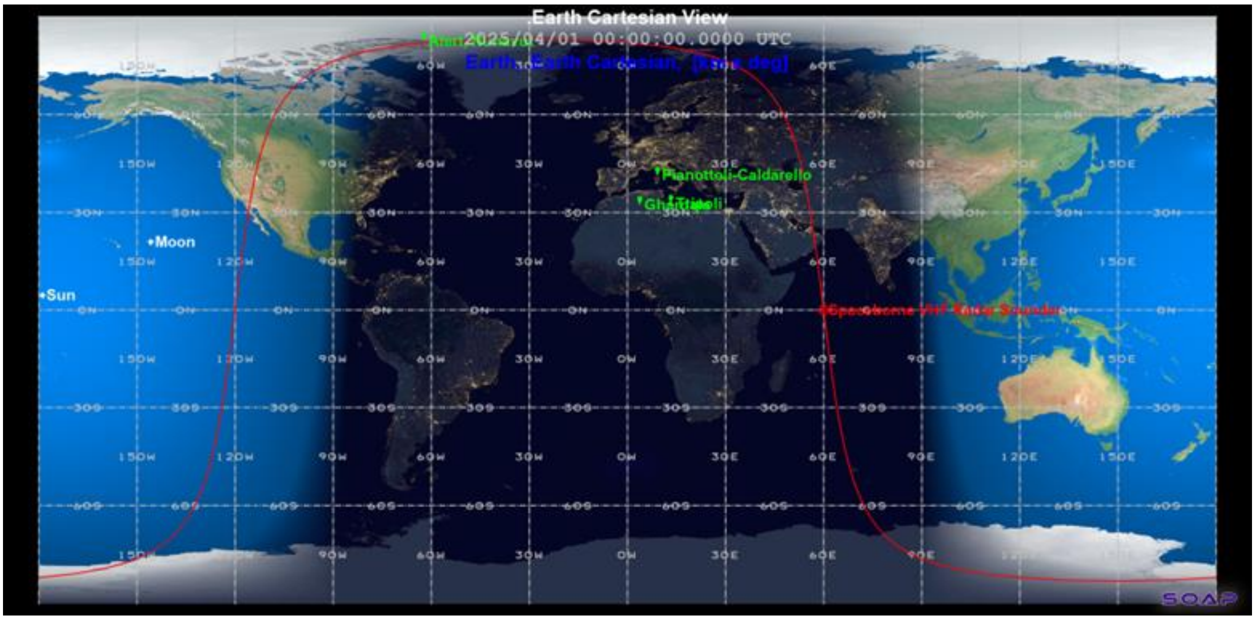

As stated in § 4.1.2, the city, residential and rural environmental types of external noise PSD levels quantified in Table 6 were considered in all sharing study simulations in this Report.

It should be noted that the percentage of time applied in the incumbent service studies should not necessarily be construed as a characterization of how much the incumbent IPC may be exceeded since in some cases the incumbent IPC is not specified as a percentage of time (e.g. applies 100% of the time).

The results of studies using the peak power in combination with OTR in equation (9) can be found in Annex 1. In Annex 2, it can be found the results of studies for the sharing and compatibility in between the radar sounder and other non-radar systems using the mean power and the OTR in equation (10).

Annex 3 presents the determination of the pfd of the radar sounder including also the calculation of a pfd for the protection of incumbent services.

6 Summary of the results of sharing studies

The sharing studies contained in this report focused on sharing and compatibility of the spaceborne VHF radar sounder under investigation with respect to the incumbent services, both within its 40-50 MHz occupied bandwidth as well as in adjacent bands.

For all the incumbent services under consideration, the potential for Interference Exceedance Level (IEL) has been assessed, assuming either:

– That peak power (Annex 1) applies for the studies or

– That mean power (Annex 2) applies for the studies, taking into account that spaceborne VHF radar sounders are pulsed radar systems.

It should be noted that the results presented in this study only considered interference from a single radar sounder and did not take into account aggregate interference effects from multiple sounders.

In the summary, the results indicate that in both static and dynamic study scenarios analysed, the operation of VHF radar sounder will exceed the interference protection criteria of most of the incumbent services.

To better understand the extent and duration of 0 dB violations of the IEL, dynamic analyses of the IEL RFI metric were carried out. The percentage of time applied in the incumbent service studies should not necessarily be construed as a characterization of how much the incumbent IPC may be exceeded since in some cases the incumbent IPC is not specified as a percentage of time (e.g. applies 100% of the time).

These results are summarised in Table 8 for the most representative sharing scenarios studied in this Report.

TABLE 8

Summary of studies for the most representative sharing scenarios

	Peak power-based interference analysis (Annex 1)		**Mean power-based interference analysis (Annex 2)**		
Victim scenario description	**Percentage of time of IPC exceedance (%)**	**Maximum IEL (dB)**	**Percentage of time of IPC exceedance (%)**	**Maximum IEL (dB)**	**Sharing considerations**
FIXED (rural)	0.1895 (Ghardaïa) 1.2324 (Alert)	27.01 (Ghardaïa) 26.70 (Alert)	0.0156	9.6654	Occurrences of interference where the incumbent IPC was exceeded. Mitigation required for EESS (active) (e.g. pfd limits and/or operational limits).
MOBILE (−10 dB IPC) (rural)	0.2456 (Ghardaïa) 1.4868 (Alert)	28.69 (Ghardaïa) 28.39 (Alert)	0.0226	12.7582	Occurrences of interference where the incumbent IPC was exceeded. Mitigation required for EESS (active) (e.g. pfd limits and/or operational limits).
MOBILE (−6 dB IPC) (rural)	0.1702 (Ghardaïa) 1.1294 (Alert)	24.69 (Ghardaïa) 24.39 (Alert)	0.0143	8.6	Occurrences of interference where the incumbent IPC was exceeded. Mitigation required for EESS (active) (e.g. pfd limits and/or operational limits).
BROADCASTING (DRM) (rural)	0.2794 (Ghardaïa) 1.4868 (Alert)	42.27 (Ghardaïa) 41.96 (Alert)	0.0484	20.6154	Occurrences of interference where the incumbent IPC was exceeded. Mitigation required for EESS (active) (e.g. pfd limits and/or operational limits). Sharing may be feasible due to the working hours of the radar sounder (maximum from 2 a.m. till 6 a.m. local time)

TABLE 8 *(end)*

	Peak power-based interference analysis (Annex 1)		Mean power-based interference analysis (Annex 2)		
Victim scenario description	**Percentage of time of IPC exceedance (%)**	**Maximum IEL (dB)**	**Percentage of time of IPC exceedance (%)**	**Maximum IEL (dB)**	**Sharing considerations**
Space research (rural)	0.0165 (Ghardaïa) 0.1618 (Alert)	19.34 (Ghardaïa) 19.04 (Alert)	0	< 0	Occurrences of interference where the incumbent IPC was exceeded for the peak power. Mitigation may be required, also noting that no SRS use has been reported in this band.
Radiolocation (rural)	0.2613 (Ghardaïa) 1.5489 (Alert)	30.97 (Ghardaïa) 30.66 (Alert)	0.0156	9.6654	Occurrences of interference where the incumbent IPC was exceeded. Mitigation required for EESS (active) (e.g. pfd limits and/or operational limits).
Oceanographic radar (rural)	0.0616	15.51	0.0510	13.4549	Occurrences of interference where the incumbent IPC was exceeded. Mitigation required for EESS (active) (e.g. pfd limits and/or operational limits).
WPR, Rec. ITU-R M.1226, (0°, 0°) (rural)	0.2624	70.56	0.2002	68.5561	Due to the limited deployment of WPR in this band, cases of harmful interference may be addressed via case-by-case coordination between concerned administrations
AMATEUR (rural)	0 (Ghardaïa) 0 (Alert)	−0.88 (Ghardaïa) –1.19 (Alert)	0	< 0	Assuming sufficient attenuation of out-of-band power, the incumbent IPC is not exceeded.

Furthermore, pfd limits have been calculated in Annex 3 that could be applied to the VHF radar sounder for the protection of the incumbent services.

Annex 1

Sharing and compatibility studies using the peak power based interference analysis

A1.1 Worst case scenario type link budget static analysis results

As the active sensor onboard the spaceborne VHF radar sounder characterized in Recommendation ITU-R RS.2042 and parameterized in Table 1 is oriented towards Earth nadir, when the sounder is directly above a victim system, the interference from the sounder will be at a maximum, assuming that receiver antenna gain effects have not been accounted for. The reason for this is that when the sounder is directly above a victim system at zenith, the transmit antenna gain G_{TX} from equation (3) will be at its maximum, the free space path loss $FSPL$ from equation (6) will be at its minimum, and the miscellaneous propagation path loss factor $L_{P,\text{misc}}$ from equation (6) will be at its minimum. Consequently, outside of victim receiver antenna gain G_{RX} orientation effects, when the sounder is directly above a victim system receiver, this constitutes a theoretical worst case scenario type condition for interference.

To refine such an analysis when the victim receiver antenna is assumed to be a half-wave dipole as described in § 4.1.1, with a certain off-zenith tilt angle β, the setup shown in Fig. A1-1 can be considered, in which the sounder is coplanar with the dipole antenna and the centre of the Earth, and at an elevation angle of δ from the victim location to the interferer position. Here, R_E is the radius of the Earth and h is the altitude of the sounder. Also, d is the distance between the sounder interferer and the incumbent service victim, while α is the off-axis angle for the victim dipole antenna. As the sounder transmit antenna gain pattern is circularly symmetric and only a function of the off-boresight angle θ as shown in Fig. 1, the maximum amount of interference will occur when the sounder is coplanar with the dipole antenna and centre of the Earth at a particular elevation angle, say $\delta_\star$.

FIGURE A1-1

Refined setup for static analysis assuming a half-wave dipole for the victim receiver antenna at a tilt angle of β

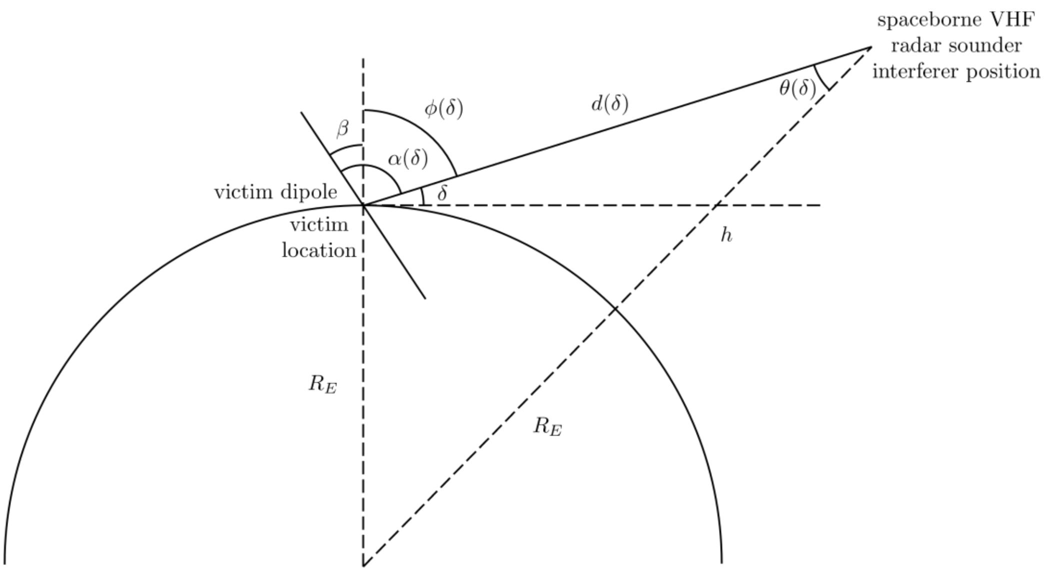

The components of the peak interference power P_r from equation (3), and subsequently the observed I/N ratio $(I/N)_{\text{obs}}$ from equation (2) and the IEL from equation (1), which depend upon the elevation angle δ from Fig. A1-1 are the interferer transmitter antenna gain $G_{TX}(\theta(\delta))$, the victim receiver antenna gain $G_{RX}(\alpha(\delta))$, the free space path loss $FSPL(d(\delta))$, and the miscellaneous losses due to ionospheric absorption $L_{P,\text{misc}}(\varphi(\theta))$. This manifests in the form $G_{TX}(\theta(\delta)) + G_{RX}(\alpha(\delta)) - FSPL(d(\delta)) - L_{P,\text{misc}}(\varphi(\theta))$ when calculating the peak interference power P_r. Thus, by finding the optimal elevation angle $\delta_\star$ where this objective function reaches its maximum value, one can obtain a more refined bound for the maximum amount of interference to be expected from the spaceborne VHF radar sounder.

Assuming a tilt angle β of 5 degrees and using the parameters for the spaceborne VHF radar sounder as in Table 1, along with the transmit antenna gain response as in Fig. 1, a plot of the objective function $G_{TX}(\theta(\delta)) + G_{RX}(\alpha(\delta)) - FSPL(d(\delta)) - L_{P,\text{misc}}(\varphi(\theta))$ as a function of the elevation angle δ is as shown in Fig. A1-2, for a nominal ionospheric absorption loss at vertical incidence of $L_{P,\text{abs;nom}} = 0.1$ dB. From this Figure, the following is obtained:

$\delta_\star = 65.71°, G_{TX}(\theta(\delta_\star)) + G_{RX}(\alpha(\delta_\star)) - FSPL(d(\delta_\star)) - L_{P,\text{misc}}(\varphi(\delta_\star)) = -117.03$ dB;

$\theta(\delta_\star) = 22.78° \Longrightarrow G_{TX}(\theta(\delta_\star)) = 7.03$ dBi;

$\alpha(\delta_\star) = 29.29° \Longrightarrow G_{RX}(\alpha(\delta_\star)) = -5.64$ dBi;

$d(\delta_\star) = 436.25 \text{ km} \Longrightarrow FSPL(d(\delta_\star)) = 118.31$ dB;

$\varphi(\delta_\star) = 24.29° \Longrightarrow L_{P,\text{misc}}(\varphi(\delta_\star)) = 0.11$ dB.

FIGURE A1-2

Plot of the peak interference power objective $G_{TX}(\theta(\delta)) + G_{RX}(\alpha(\delta)) - FSPL(d(\delta)) - L_{P,\text{misc}}(\varphi(\theta))$ as a function of the victim to interferer elevation angle δ, with the optimal value identified, assuming $L_{P,\text{abs;nom}} = 0.1$ dB

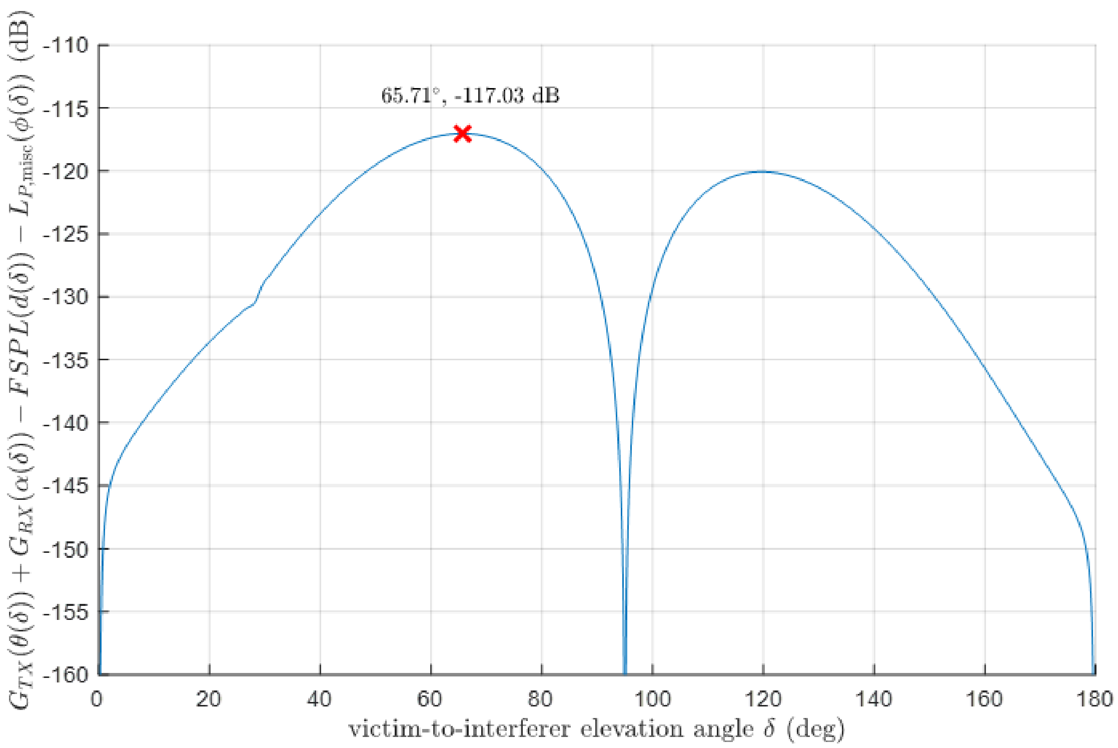

Using these results, a link budget based static analysis was carried out to assess whether or not there is compliance with respect to the IPC for a particular incumbent service system, which is equivalent to determining whether or not the IEL from equation (1) is below or above the 0 dB threshold. In Table A1-1, various parameters used for the spaceborne VHF radar sounder worst case static RFI analysis are listed.

TABLE A1-1

Various parameters used for the spaceborne VHF radar sounder worst case scenario static RFI analysis for the case of a half-wave dipole antenna for the victim receiver at a tilt angle of 5 degrees

Parameter	Value
P_{TX}	20 dBW
$G_{TX}\big(\theta(\delta_\star)\big)$	7.03 dBi
$G_{RX}\big(\alpha(\delta_\star)\big)$	−5.64 dBi
L_{TX}	0 dBi
$FSPL\big(d(\delta_\star)\big)$	118.31 dB
$L_{P,\mathrm{misc}}\big(\varphi(\delta_\star)\big)$	0.11 dB
B_c	10 MHz (nominal),
τ	85 μs
$OFR(\Delta f)$	0 dB

Using the parameter values given in Table A1-1, the results for the worst case scenario static RFI analysis are shown in Table A1-2. In this table are listed the victim receiver bandwidth B_r and the bandwidth of the transmitter spectrum appearing in the victim receiver bandwidth $B_{t\ \mathrm{in}\ r}$. These values come from the subsequent sections which contain the results of further refined dynamic RFI analyses.

TABLE A1-2

Worst case scenario static RFI analysis results to assess the impact of the spaceborne VHF radar sounder characterized in Recommendation ITU-R RS.2042 with respect to incumbent service systems

Typical ionospheric absorption (0.1 dB at vertical incidence at 45 MHz)							
Incumbent service system	**Constant loss factors** $L_{TX} + L_{RX} + L_{P,\mathrm{pol}}$ **(dB)**	B_r **(kHz)**	$B_{t\ \mathrm{in}\ r}$ **(kHz)**	OTR **(dB)**	$(I/N)_{\mathrm{IPC}}$ **(dB)**	**Static analysis maximum received peak interference power** P_r **(dBW)**	**Static analysis** IEL **(dB)**
FIXED	0	36	36	19.58	−6	−116.60	16.72 (city), 20.88 (residential), 25.68 (rural)
MOBILE (−6 dB *I*/*N* IPC)	4	75	75	13.20	−6	−114.23	15.90 (city), 20.04 (residential), 24.81 (rural)
MOBILE (−10 dB *I*/*N* IPC)	4	75	75	13.20	−10	−114.23	19.90 (city), 24.04 (residential), 28.81 (rural)
BROADCASTING (DRM)	3	96	96	11.06	−20	−111.09	31.98 (city), 36.14 (residential), 40.94 (rural)
BROADCASTING (ST61 TV)	3	8 000	2 500	0	−20	−100.03	23.83 (city), 27.99 (residential), 32.79 (rural)

TABLE A1-2 *(end)*

Typical ionospheric absorption (0.1 dB at vertical incidence at 45 MHz)							
Incumbent service system	**Constant loss factors $L_{TX}+L_{RX}+L_{P,\text{pol}}$ (dB)**	**B_r (kHz)**	**$B_{t\text{ in }r}$ (kHz)**	**OTR (dB)**	**$(I/N)_{\text{IPC}}$ (dB)**	**Static analysis maximum received peak interference power P_r (dBW)**	**Static analysis IEL (dB)**
Radiolocation	0	125	125	8.77	−6	−105.79	22.12 (city), 26.28 (residential), 31.09 (rural)
Space research	0	1	1	50.71	−6	−138.36	10.52 (city), 14.68 (residential), 19.49 (rural)
AMATEUR in 50-54 MHz, (EESS active nominal mask)	4	16	0	20 (OOB attenuation factor)	−6	−148.01	−11.17 (city), −7.01 (residential), −2.21 (rural)
AMATEUR in 50-54 MHz, (EESS active with Rec. ITU-R SM.1541-6 spectral mask)	4	16	16	29.48	−6	−130.51	6.33 (city), 10.49 (residential), 15.30 (rural)

It should be noted that the results present in Table A1-2 reflect a true worst case scenario setting in which all effects due to angular dependent propagation losses, constant loss factors due to transmission/feeder losses and polarization mismatch, and internal victim receiver noise have been accounted for. From this Table, it can be seen that the IEL in all cases exceeded the 0 dB threshold for harmful interference. This served as the impetus to consider dynamic simulations of the RFI to better assess the degree of interference effects of the spaceborne VHF radar sounder upon the incumbent service systems under consideration in this sharing studies report, in particular the percentage of time over which the IEL exceeds the 0 dB threshold.

A1.2 In-band primary service dynamic analysis based sharing studies

The set of spaceborne VHF radar sounder interferer parameters relevant to calculating the IEL that were used throughout all of the dynamic simulations contained in this Report are given in Table A1-3. To compute the transmit antenna gain G_{TX}, the gain pattern from Fig. 2 was used exclusively.

TABLE A1-3

Parameters for the spaceborne VHF radar sounder used throughout all dynamic RFI simulation sharing studies

Quantity	Units	Value
P_{TX}	dBW	20
L_{TX}	dB	0
B_c	MHz	10
τ	μs	85

A1.2.1 Fixed service dynamic analysis based sharing studies

Over the 40-50 MHz VHF band of interest, there are no technical characteristics for systems operating in the fixed service in the ITU-R recommendations. As such, a nominal set of parameters was used for the dynamic RFI simulations. Specifically, no internal noise source was considered, a half-wave dipole antenna gain pattern was assumed for the receiver antenna (with two possible tilt angles), and no losses were attributed to polarization mismatch or receiver hardware effects. Based on these assumptions and the data from Table 3, the relevant quantities used for the fixed service sharing studies are given in Table A1-4.

TABLE A1-4

Parameters used in dynamic RFI simulation sharing studies to assess the impact of the spaceborne VHF radar sounder upon the in-band fixed service

Quantity	Units	Value
$(I/N)_{\text{IPC}}$	dB	−6
B_r	kHz	36
$B_{t\ \text{in}\ r}$	kHz	36
NF	dB	0

TABLE A1-4 *(end)*

Quantity	Units	Value
G_{RX}	half-wave dipole (equation (5)), tilt angles β of 5° and 10°	
$L_{P,\text{pol}}$	dB	0
L_{RX}	dB	0

The maximum received peak interference power P_r, the maximum IEL observed, and the percentage of time that the IEL exceeded 0 dB, for each noise environmental category for the fixed service sharing study, are shown in Table A1-5.

TABLE A1-5

Maximum received peak interference power and IEL values, along with the IEL 0 dB exceedance percentage of time, for the in-band fixed service sharing study set (assuming transmission $D_{op} \times 100\%$ = 10.79% of the time)

Environmental category	Receiver antenna tilt angle (degrees)	Dynamic analysis maximum received peak interference power P_r (dBW)	Dynamic analysis maximum IEL (dB)	Percentage of time IEL exceeds 0 dB (%)
City	5	−116.73 (Ghardaïa) −117.03 (Alert)	16.60 (Ghardaïa) 16.29 (Alert)	0.0426 (Ghardaïa) 0.3290 (Alert)
Residential	5		20.76 (Ghardaïa) 20.45 (Alert)	0.0891 (Ghardaïa) 0.6000 (Alert)
Rural	5		25.56 (Ghardaïa) 25.26 (Alert)	0.1918 (Ghardaïa) 1.2467 (Alert)
City	10	−115.28 (Ghardaïa) −115.59 (Alert)	18.04 (Ghardaïa) 17.73 (Alert)	0.0417 (Ghardaïa) 0.3292 (Alert)
Residential	10		22.20 (Ghardaïa) 21.89 (Alert)	0.0874 (Ghardaïa) 0.5931 (Alert)
Rural	10		27.01 (Ghardaïa) 26.70 (Alert)	0.1895 (Ghardaïa) 1.2324 (Alert)

A1.2.2 Mobile service dynamic analysis based sharing studies

Technical and operational characteristics for mobile systems operating over the 40-50 MHz VHF band of interest can be found in Recommendation ITU-R M.1808-1. Specifically, Table 1A includes characteristics for analogue and digital systems operating over the 30-88 MHz frequency range. Based on the values present in this table, the relevant quantities used for the mobile service sharing studies are given in Table A1-6. Here, the polarization loss of 3 dB is attributed to the mismatch between the spaceborne VHF radar sounder circular polarization (see Table 1) and the mobile system vertical polarization (see Table 1A of Recommendation ITU-R M.1808-1).

TABLE A1-6

Parameters used in dynamic RFI simulation sharing studies to assess the impact of the spaceborne VHF radar sounder upon the in-band mobile service

Quantity	Units	Value
$(I/N)_{\text{IPC}}$	dB	−6, −10
B_r	kHz	75
$B_{t\text{ in }r}$	kHz	75
NF	dB	5
G_{RX}	half-wave dipole (equation (5)), tilt angles β of 0° and 5°	
$L_{P,\text{pol}}$	dB	3
L_{RX}	dB	1

The maximum received peak interference power P_r, the maximum IEL observed, and the percentage of time that the IEL exceeded 0 dB, for each noise environmental category for the mobile service sharing study, are shown in Table A1-7.

TABLE A1-7

Maximum received peak interference power and IEL values, along with the IEL 0 dB exceedance percentage of time, for the in-band mobile service sharing study set (assuming transmission $D_{op} \times 100\%$ = 10.79% of the time)

Environmental category	Receiver antenna tilt angle (degrees)	Dynamic analysis maximum received peak interference power P_r (dBW)	Dynamic analysis maximum IEL (dB)	Percentage of time IEL exceeds 0 dB (%)
City (−6 dB *I*/*N* IPC)	0	−115.92 (Ghardaïa) −116.23 (Alert)	14.21 (Ghardaïa) 13.90 (Alert)	0.0368 (Ghardaïa) 0.2899 (Alert)
Residential (−6 dB *I*/*N* IPC)	0		18.36 (Ghardaïa) 18.05 (Alert)	0.0780 (Ghardaïa) 0.5352 (Alert)
Rural (−6 dB *I*/*N* IPC)	0		23.12 (Ghardaïa) 22.81 (Alert)	0.1713 (Ghardaïa) 1.1397 (Alert)
City (−6 dB *I*/*N* IPC)	5	−114.35 (Ghardaïa) −114.65 (Alert)	15.78 (Ghardaïa) 15.47 (Alert)	0.0363 (Ghardaïa) 0.2905 (Alert)
Residential (−6 dB *I*/*N* IPC)	5		19.92 (Ghardaïa) 19.62 (Alert)	0.0772 (Ghardaïa) 0.5318 (Alert)
Rural (−6 dB *I*/*N* IPC)	5		24.69 (Ghardaïa) 24.39 (Alert)	0.1702 (Ghardaïa) 1.1294 (Alert)

TABLE A1-7 *(end)*

Environmental category	Receiver antenna tilt angle (degrees)	Dynamic analysis maximum received peak interference power P_r (dBW)	Dynamic analysis maximum IEL (dB)	Percentage of time IEL exceeds 0 dB (%)
City (−10 dB *I*/*N* IPC)	0	−115.92 (Ghardaïa) −116.23 (Alert)	18.21 (Ghardaïa) 17.90 (Alert)	0.0762 (Ghardaïa) 0.5238 (Alert)
Residential (−10 dB *I*/*N* IPC)	0		22.36 (Ghardaïa) 22.05 (Alert)	0.1525 (Ghardaïa) 1.0190 (Alert)
Rural (−10 dB *I*/*N* IPC)	0		27.12 (Ghardaïa) 26.81 (Alert)	0.2460 (Ghardaïa) 1.4882 (Alert)
City (−10 dB *I*/*N* IPC)	5	−114.35 (Ghardaïa) −114.65 (Alert)	19.78 (Ghardaïa) 19.47 (Alert)	0.0754 (Ghardaïa) 0.5205 (Alert)
Residential (−10 dB *I*/*N* IPC)	5		23.92 (Ghardaïa) 23.62 (Alert)	0.1512 (Ghardaïa) 0.9987 (Alert)
Rural (−10 dB *I*/*N* IPC)	5		28.69 (Ghardaïa) 28.39 (Alert)	0.2456 (Ghardaïa) 1.4868 (Alert)

A1.2.3 Broadcasting service dynamic analysis based sharing studies

Characteristics for specific systems operating in the broadcasting service over the 30-3 000 MHz frequency range (which includes the 40-50 MHz VHF band of interest) can be found in Recommendation ITU-R BS.1114-12. Specifically, the Digital Radio Mondiale (DRM) system operating in the broadcasting service over the 47-68 MHz band is defined and characterized in this recommendation. A lesser used but still relevant broadcasting service is the Stockholm Frequency Plan of 1961 (ST61). Over the 47-68 MHz frequency range (VHF Band I for the broadcasting service), ST61 contains 768 recorded analogue television (TV) stations with bandwidth of 7 and 8 MHz, as well as 377 sound broadcasting stations with bandwidths of 130 and 180 kHz. More information about the broadcasting service in the VHF Band I can also be found in Electronic Communications Committee (ECC) Report 117: Managing the transition to digital sound broadcasting in the frequency bands below 80 MHz.

It should be noted that the ST61 TV stations with 7 and 8 MHz bandwidth over the 47-68 MHz band have partial spectral overlap with the spaceborne VHF radar sounder operating over the 40-50 MHz frequency range. As such, the receiver filter bandwidth B_r and the 3 dB bandwidth of the transmitter emission appearing in the receiver filter bandwidth $B_{t\text{ in }r}$, also referred to as the interfered receiver 3 dB bandwidth, will differ from each other in this case. From Fig. 4, with the 8 MHz 3 dB bandwidth of the spaceborne VHF radar sounder being over the 41-49 MHz band, an ST61 TV station over the band 47-68 MHz would correspond to a value of $B_{t\text{ in }r} = 2\ 000$ kHz, although a more accurate value would be 2 500 kHz, which was used in the sharing studies of this Report.

For sake of completeness, to assess the impact of the characteristic spaceborne VHF radar sounder on the in-band broadcasting primary service, two such victim types were considered: a DRM system along with a TV system in accordance with the ST61 band plan. The relevant quantities used for the broadcasting service sharing studies are given in Table A1-8.

TABLE A1-8

Parameters used in dynamic RFI simulation sharing studies to assess the impact of the spaceborne VHF radar sounder upon the in-band broadcasting service (DRM and ST61 TV systems considered)

Quantity	Units	Value	
		DRM	ST61 TV
$(I/N)_{\text{IPC}}$	dB	−20	−20
B_r	kHz	96	8 000
$B_{t \text{ in } r}$	kHz	96	2 500
NF	dB	0	0
G_{RX}	half-wave dipole (equation (5)), tilt angles β of 5° and 10°		
$L_{P,\text{pol}}$	dB	3	3
L_{RX}	dB	0	0

The maximum received peak interference power P_r, the maximum IEL observed, and the percentage of time that the IEL exceeded 0 dB, for each noise environmental category for the broadcasting service sharing study, are shown in Table A1-9.

TABLE A1-9

Maximum received peak interference power and IEL values, along with the IEL 0 dB exceedance percentage of time, for the in-band broadcasting service sharing study set (assuming transmission $D_{op} \times 100\%$ = 10.79% of the time)

Environmental category	Receiver antenna tilt angle (degrees)	Dynamic analysis maximum received peak interference power P_r (dBW)	Dynamic analysis maximum IEL (dB)	Percentage of time IEL exceeds 0 dB (%)
City (DRM)	5	−111.21 (Ghardaïa) −111.51 (Alert)	31.86 (Ghardaïa) 31.55 (Alert)	0.2649 (Ghardaïa) 1.5632 (Alert)
Residential (DRM)	5		36.01 (Ghardaïa) 35.71 (Alert)	0.2746 (Ghardaïa) 1.5995 (Alert)
Rural (DRM)	5		40.82 (Ghardaïa) 40.52 (Alert)	0.2795 (Ghardaïa) 1.6176 (Alert)
City (DRM)	10	−109.76 (Ghardaïa) −110.07 (Alert)	33.30 (Ghardaïa) 32.99 (Alert)	0.2646 (Ghardaïa) 1.5621 (Alert)
Residential (DRM)	10		37.46 (Ghardaïa) 37.15 (Alert)	0.2745 (Ghardaïa) 1.5991 (Alert)
Rural (DRM)	10		42.27 (Ghardaïa) 41.96 (Alert)	0.2794 (Ghardaïa) 1.6174 (Alert)

TABLE A1-9 *(end)*

Environmental category	**Receiver antenna tilt angle (degrees)**	**Dynamic analysis maximum received peak interference power P_r (dBW)**	**Dynamic analysis maximum IEL (dB)**	**Percentage of time IEL exceeds 0 dB (%)**
City (ST61 TV)	5	−100.15 (Ghardaïa) −100.45 (Alert)	23.71 (Ghardaïa) 23.40 (Alert)	0.1461 (Ghardaïa) 0.9536 (Alert)
Residential (ST61 TV)	5		27.87 (Ghardaïa) 27.56 (Alert)	0.2358 (Ghardaïa) 1.4473 (Alert)
Rural (ST61 TV)	5		32.67 (Ghardaïa) 32.37 (Alert)	0.2677 (Ghardaïa) 1.5737 (Alert)
City (ST61 TV)	10	−98.70 (Ghardaïa) −99.01 (Alert)	25.15 (Ghardaïa) 24.85 (Alert)	0.1436 (Ghardaïa) 0.9282 (Alert)
Residential (ST61 TV)	10		29.31 (Ghardaïa) 29.00 (Alert)	0.2349 (Ghardaïa) 1.4423 (Alert)
Rural (ST61 TV)	10		34.12 (Ghardaïa) 33.81 (Alert)	0.2674 (Ghardaïa) 1.5729 (Alert)

A1.3 In-band secondary service dynamic analysis based sharing studies

Sharing studies for secondary services which are in-band with respect to the 40-50 MHz frequency band spanned by the spaceborne VHF radar sounder were carried out similarly to those done in § A1.2. Specifically, the city of Ghardaïa, Algeria and the area of Alert, Nunavut were chosen as the victim locations, and the dynamic RFI simulations took place over the 18-month observation epoch using a 5-second time increment.

The exceptions to this were the oceanographic radar and wind profiler radar case studies covered in §§ A1.3.1.1 and A1.3.1.2, respectively. These systems, which fall under the radiolocation service, are characterized in more detail in the ITU-R Recommendations than other services in the target VHF band. As such, special attention was given to them. In particular, the dynamic RFI simulation setup was slightly modified in each case to better reflect the operations of such systems in a more realistic setting.

A1.3.1 Radiolocation service sharing studies

Along with the fixed and broadcasting service sharing studies, over the 40-50 MHz VHF band of interest, there are no technical characteristics for generic systems operating in the radiolocation service in the ITU-R Recommendations. As such, a nominal set of parameters was used for the dynamic RFI simulations. Specifically, no internal noise source was considered, a half-wave dipole antenna gain pattern was assumed for the receiver antenna (with two possible tilt angles), and no losses were attributed to polarization mismatch or receiver hardware effects. Based on these assumptions and the data from Table 3, the relevant quantities used for the radiolocation service sharing studies are given in Table A1-10.

TABLE A1-10

Parameters used in dynamic RFI simulation sharing studies to assess the impact of the spaceborne VHF radar sounder upon the in-band radiolocation service

Quantity	Units	Value
$(I/N)_{\text{IPC}}$	dB	−6
B_r	kHz	125
$B_{t\text{ in }r}$	kHz	125
NF	dB	0
G_{RX}	half-wave dipole (equation (5)), tilt angles β of 0° and 5°	
$L_{P,\text{pol}}$	dB	0
L_{RX}	dB	0

The maximum received peak interference power P_r, the maximum IEL observed, and the percentage of time that the IEL exceeded 0 dB, for each noise environmental category for the radiolocation service sharing study, are shown in Table A1-11.

TABLE A1-11

Maximum received peak interference power and IEL values, along with the IEL 0 dB exceedance percentage of time, for the in-band radiolocation service sharing study set (assuming transmission $D_{op} \times 100\%$ = 10.79% of the time)

Environmental category	Receiver antenna tilt angle (degrees)	Dynamic analysis maximum received peak interference power P_r (dBW)	Dynamic analysis maximum IEL (dB)	Percentage of time IEL exceeds 0 dB (%)
City	0	−107.48 (Ghardaïa) −107.79 (Alert)	20.44 (Ghardaïa) 20.12 (Alert)	0.1110 (Ghardaïa) 0.7301 (Alert)
Residential	0		24.60 (Ghardaïa) 24.28 (Alert)	0.2067 (Ghardaïa) 1.3195 (Alert)
Rural	0		29.40 (Ghardaïa) 29.09 (Alert)	0.2615 (Ghardaïa) 1.5494 (Alert)
City	5	−105.91 (Ghardaïa) −106.22 (Alert)	22.00 (Ghardaïa) 21.70 (Alert)	0.1099 (Ghardaïa) 0.7225 (Alert)
Residential	5		26.16 (Ghardaïa) 25.86 (Alert)	0.2059 (Ghardaïa) 1.3143 (Alert)
Rural	5		30.97 (Ghardaïa) 30.66 (Alert)	0.2613 (Ghardaïa) 1.5489 (Alert)

A1.3.1.1 Oceanographic radar system sharing studies

In this section is considered a case study to assess the impact of the spaceborne VHF radar sounder upon a set of characteristic oceanographic radar systems in the radiodetermination service over the 3-50 MHz band, which are described in Recommendation ITU-R M.1874-1. From RR No. **5.132A** of the Radio Regulations (RR) Edition of 2020, the band 42-42.5 MHz is allocated to the radiolocation service on a secondary basis, the use of which is limited to oceanographic radars in accordance with Resolution **612 (WRC-12)**.

Characteristics of oceanographic radars at 42 MHz

Technical and operational characteristics for oceanographic radar systems in the radiodetermination service over the band 3-50 MHz are described in Recommendation ITU-R M.1874-1. Among the specific systems parameterized, there are three in the 40-50 MHz band:

– System 4 (Table 2 of Recommendation ITU-R M.1874-1):
  - Centre frequency: 42 MHz,
  - Modulation type: frequency modulated interrupted continuous wave (FMICW).
– System 9 (Table 3 of Recommendation ITU-R M.1874-1):
  - Centre frequency: 42 MHz,
  - Modulation type: frequency modulated continuous wave (FMCW).
– System 13 (Table 4 of Recommendation ITU-R M.1874-1):
  - Centre frequency: 41.9 MHz,
  - Modulation type: not specified.

As the receiver intermediate frequency (IF) 3 dB bandwidth, a necessary parameter for this analysis, was not specified for System 13 in Recommendation ITU-R M.1874-1, only Systems 4 and 9 were considered here for the dynamic RFI simulations. This may be satisfactory for this analysis, as the parameters for System 13 appear to be less susceptible to RFI than those for System 9.

Parameters relevant to the dynamic RFI simulation for System 4 are shown in Table A1-12 (taken from Table 2 of Recommendation ITU-R M.1874-1). While a receiver antenna radiation pattern was not specifically available for System 4, an omnidirectional type pattern, taken from Fig. 7 of Recommendation ITU-R M.1874-1 and reproduced here in Fig. A1-3, was used. Of the antenna radiation patterns present in Recommendation ITU-R M.1874-1 for which quantitative gain values can be extracted, it appears to be the closest fit for System 4.

TABLE A1-12

Technical and operational characteristics for 42 MHz, FMICW oceanographic radar System 4 described in Rec. ITU-R M.1874-1 (data taken from Table 2 of Rec. ITU-R M.1874-1)

Characteristics	**System 4 42 MHz**
Frequency range (MHz)	40-44
Receive antenna pattern type	Electric and magnetic dipoles
Receive antenna type	Two crossed loops and a monopole as a single unit
Receive antenna polarization	Vertical
Receive antenna main beam gain (dBi)	5
Receive antenna elevation beamwidth (degrees)	45

TABLE A1-12 *(end)*

Characteristics	**System 4** **42 MHz**
Receive antenna azimuth beamwidth (degrees)	90-360
Receive antenna horizontal scan rate	Fixed antenna
Receive antenna height (m)	4
Receiver IF 3 dB bandwidth (Hz)	500
Receiver noise figure (dB)	12 with pulsing
Minimum discernible signal (dBm)	−147 (500 Hz RBW) (specified system noise level)

FIGURE A1-3

Relative receiver antenna gain pattern used for the 42 MHz, FMICW oceanographic radar System 4 taken from Fig. 7 of Rec. ITU-R M.1874-1 (omnidirectional; left: azimuthal, right: vertical)

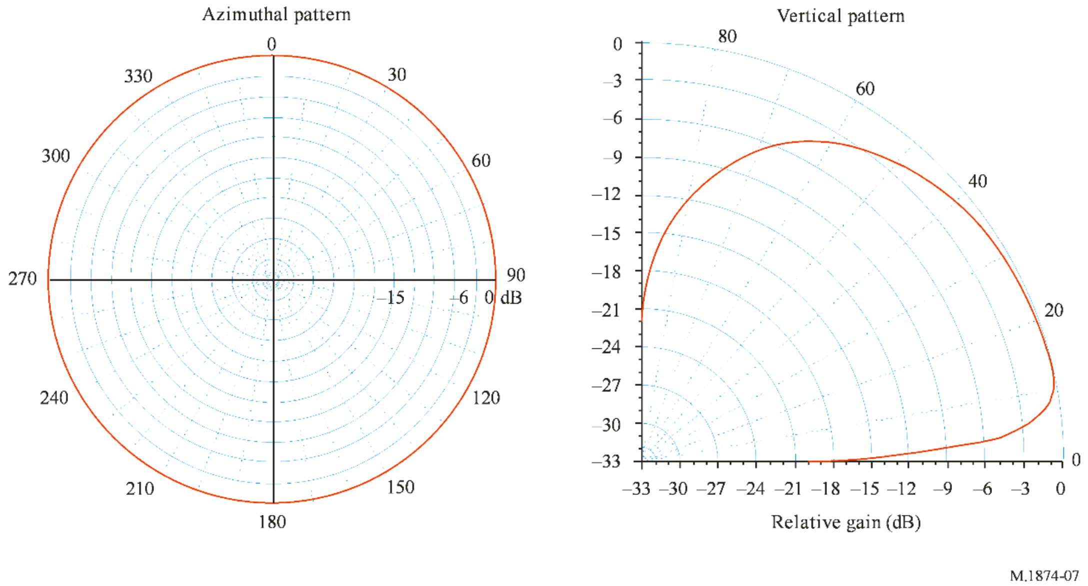

Parameters relevant to the dynamic RFI simulation for System 9 are shown in Table A1-13 (taken from Table 3 of Recommendation ITU-R M.1874-1). While a receiver antenna radiation pattern was not available for System 9, a 3-element Yagi type pattern, taken from Fig. 8 of Recommendation ITU-R M.1874-1 and reproduced here in Fig. A1-4, was used. Of the radiation patterns present in Recommendation ITU-R M.1874-1 for which quantitative gain values can be extracted, it appears to be the closest fit for System 9.

TABLE A1-13

Technical and operational characteristics for 42 MHz, FMCW oceanographic radar System 9 described in Rec. ITU-R M.1874-1 (data taken from Table 3 of Rec. ITU-R M.1874-1)

Characteristics	System 9 42 MHz
Frequency range (MHz)	40-44
Receive antenna pattern type	Directional with beamwidth ±3° to ±15°
Receive antenna type	Monopole array (4 to 16 monopoles)
Receive antenna polarization	Vertical
Receive antenna main beam gain (dBi)	10 to 18
Receive antenna elevation beamwidth (degrees)	35
Receive antenna azimuth beamwidth (degrees)	6 to 30 depending on array size
Receive antenna horizontal scan rate	Fixed antenna
Receive antenna height (m)	< 2
Receiver IF 3 dB bandwidth (kHz)	No IF used. Baseband bandwidth is 1.5
Receiver noise figure (dB)	8
Minimum discernible signal (dBm)	−142 in 1 500 Hz RBW (specified system noise level)

FIGURE A1-4

Relative receiver antenna gain pattern used for the 42 MHz, FMCW oceanographic radar System 9 taken from Fig. 8 of Rec. ITU-R M.1874-1 (directional, 3-element Yagi; left: azimuthal, right: vertical)

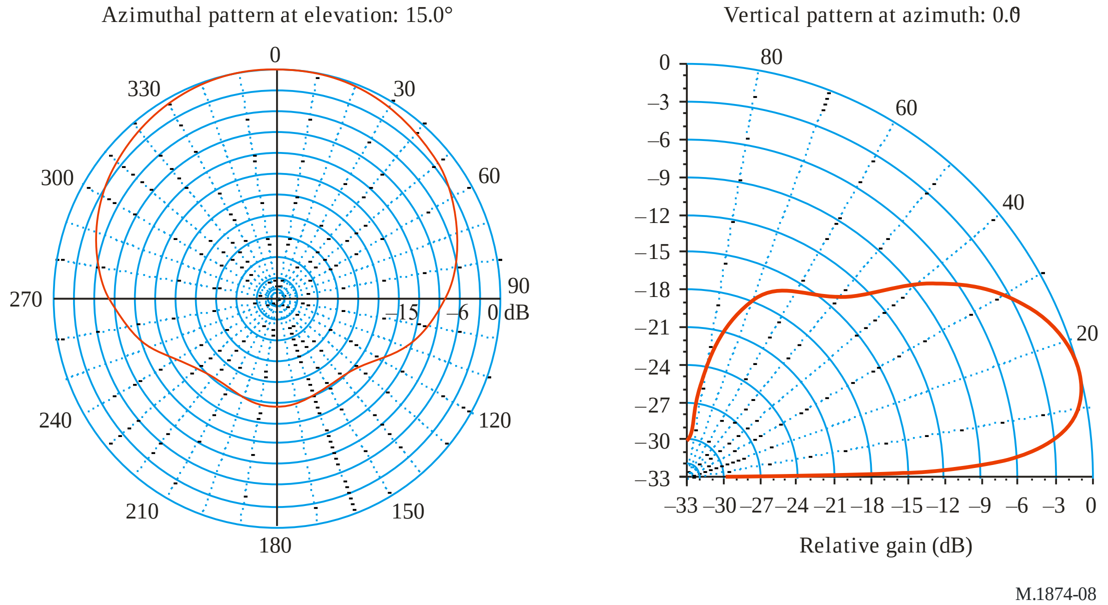

Considering both the spaceborne VHF radar sounder interferer and oceanographic radar system victims, the set of fixed quantities used in the dynamic RFI simulations for this section are shown in Table A1-14. Note that the polarization mismatch loss $L_{P,\mathrm{pol}}$ value of 3 dB is a result of the fact that the spaceborne VHF sounder employs circular polarization, while the oceanographic radar systems each use vertical polarization.

TABLEA1-14

Parameters used in dynamic RFI simulation sharing studies to assess the impact of the spaceborne VHF radar sounder upon in-band oceanographic radar systems operating in the radiolocation service

Quantity	Units	Value
$(I/N)_{\text{IPC}}$	dB	-6
B_r	kHz	0.5 (System 4), 1.5 (System 9)
$B_{t\text{ in }r}$	kHz	0.5 (System 4), 1.5 (System 9)
NF	dB	12 (System 4), 8 (System 9)
G_{RX} (peak)	dBi	5 (System 4), 18 (System 9)
$L_{P,\text{pol}}$	dB	3
L_{RX}	dB	0

Quantitative data from the relative antenna gain patterns shown in Figs A1-3 and A1-4 were not available, and instead, a best-efforts approach was used to extract the values as faithfully as possible. The results of extraction of data values are shown in Fig. A1-5, for the omnidirectional antenna pattern shown in Fig. A1-3, and in Fig. A1-6, for the directional 3-element Yagi antenna pattern shown in Fig. A1-4.

FIGURE A1-5

Results of extraction of data from the relative antenna gain pattern for the omnidirectional antenna from Fig. A1-3 (top: original, bottom: extracted results)

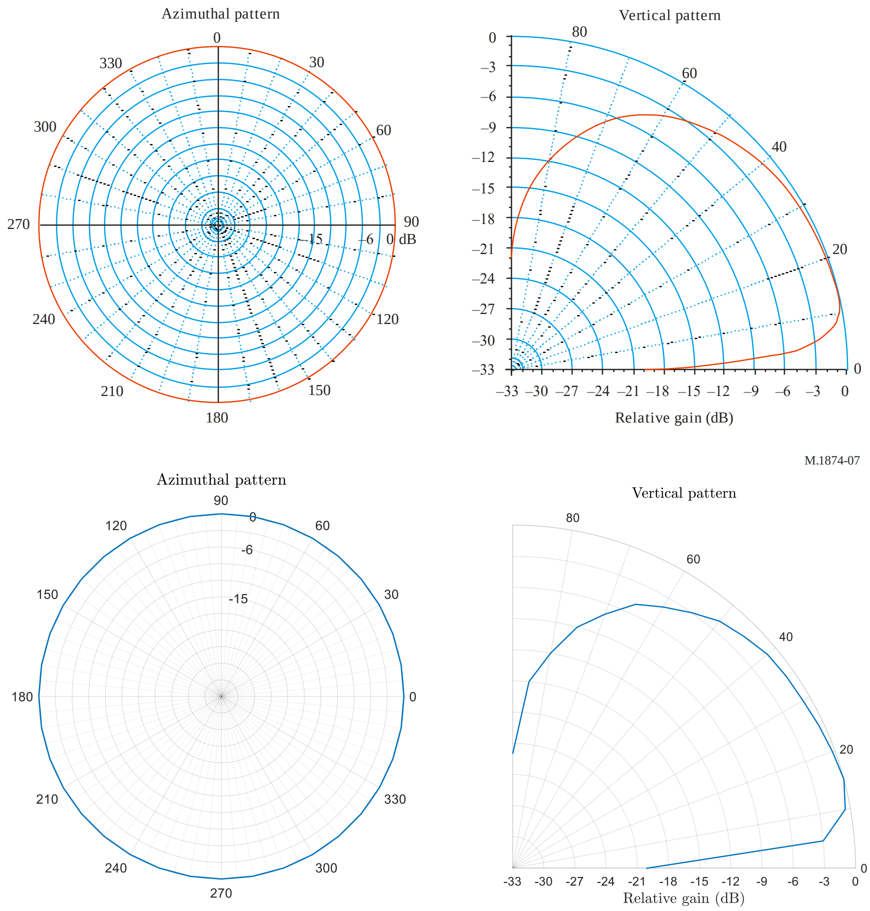

FIGURE A1-6

Results of extraction of data from the relative antenna gain pattern for the directional 3-element Yagi antenna from Fig. A1-4 (top: original, bottom: extracted results)

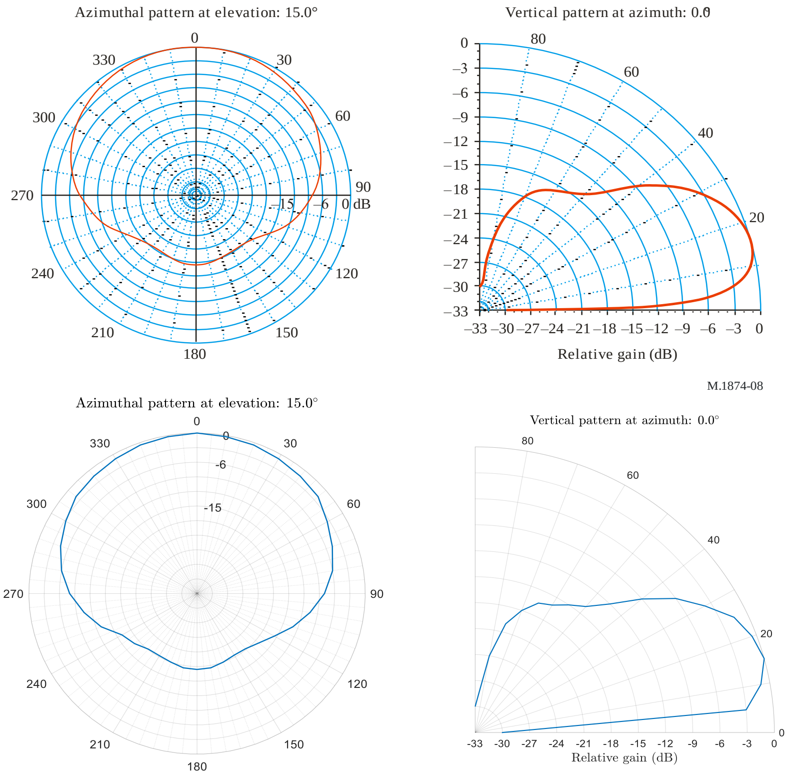

Results of dynamic RFI simulations

The maximum received peak interference power P_r, the maximum IEL observed, and the percentage of time that the IEL exceeded 0 dB, for each noise environmental category for the oceanographic radar system radiolocation service sharing study, are shown in Table A1-15.

TABLE A1-15

Maximum received peak interference power and IEL values, along with the IEL 0 dB exceedance percentage of time, for the in-band oceanographic radar system radiolocation service sharing study set (assuming transmission $D_{op} \times 100\% = 10.79\%$ of the time)

Environmental category	Dynamic analysis maximum received peak interference power P_r (dBW)	Dynamic analysis maximum IEL (dB)	Percentage of time IEL exceeds 0 dB (%)
City (System 4)	−151.45	0.39	0.0010
Residential (System 4)		4.47	0.0071
Rural (System 4)		9.03	0.0131
City (System 9)	−140.44	6.67	0.0088
Residential (System 9)		10.80	0.0301
Rural (System 9)		15.51	0.0616

A1.3.1.2 Wind profiler radar system sharing studies

From No. **5.162A** of the Radio Regulations (RR) Edition of 2020, in 32 countries (encompassing Europe, China, and the Russian Federation), the band 46-68 MHz is allocated to the radiodetermination service on a secondary basis, the use of which is limited to wind profiler radar (WPR) systems in accordance with Resolution **217 (WRC-97)**. Report ITU-R M.2013 specifies that a relatively low density of wind profiler radars is needed for frequency sharing between wind profiler radars and other incumbent services in the 40-80 MHz frequency range.

Special attention must be made to assess the level of RFI from a spaceborne interferer, as there is potential for mainlobe-to-mainlobe coupling between the interferer and victim antenna beam orientations. As such, for this case, the expected level of RFI from a given spaceborne VHF sounder will be significantly larger than for the previous cases considered.

A general overview and a set of nominal operational parameters for WPR systems are respectively given in the following set of ITU publications:

- Report ITU-R M.2013: Wind profiler radars,
- Recommendation ITU-R M.1226: Technical and operational characteristics of wind profiler radars in bands in the vicinity of 50 MHz.

In this section is considered a case study to assess the impact of the spaceborne VHF radar sounder upon a candidate WPR system operating near 50 MHz across a set of receiver antenna gain patterns and beam orientations.

Characteristics of candidate wind profiler radar operating near 50 MHz

A set of representative technical parameters for WPR systems operating in bands near 50 MHz are given in Tables 1 and 2 of Recommendation ITU-R M.1226 and shown in Table A1-16. While this Table provides a range for the maximum gain in the main beam of the antenna, a description of the antenna sidelobe suppression for specified angles above the horizon is given in Table 3 of Recommendation ITU-R M.1226 and shown in Table A1-17.

TABLE A1-16

Representative values for operational WPR parameters in the bands near 50 MHz described in Rec. ITU-R M.1226 (data taken from Tables 1 and 2 of Rec. ITU-R M.1226)

Characteristics	Values
Main beam antenna gain (dBi)	30-34
Beamwidth (degrees)	4-6
Tilt angle (degrees)	11-16
Pulse width (μs)	1-10
Necessary bandwidth (MHz)	2.2-0.2
Occupied/necessary bandwidth ratio	≤ 2.5

TABLE A1-17

Antenna sidelobe suppression values for specified angles above the horizon for WPR systems described in Rec. ITU-R M.1226 (data taken from Table 3 of Rec. ITU-R M.1226)

Angle above the horizon (degrees)	Antenna side-lobe suppression (dB)	
	Median	Minimum
0-5	40	33
5-45	30	23
> 45	23	13

To obtain a worst-case victim receiver antenna gain pattern, the following parameters were selected:

- Main bean antenna gain: 34 dBi
- Beamwidth: 6
- Tilt angle: 11
- Necessary bandwidth: 2.2 MHz
- Antenna side-lobe suppression: Minimum.

From these parameters' values, a worst-case victim receiver antenna gain pattern G_{RX} as a function of the off-boresight angle φ was constructed, as given below in equation (A1-1) and shown in Fig. A1-7.

$$G_{RX}(\varphi) = \begin{cases} 34\text{ dBi}, & 0° \leq \varphi < 3° \\ 21\text{ dBi}, & 3° \leq \varphi < 34° \\ 11\text{ dBi}, & 34° \leq \varphi < 74° \\ 1\text{ dBi}, & 74° \leq \varphi < 180° \end{cases} \quad \text{(A1-1)}$$

FIGURE A1-7

Worst-case victim receiver antenna gain pattern G_{RX} as a function of the off-boresight angle φ for a WPR operating near 50 MHz

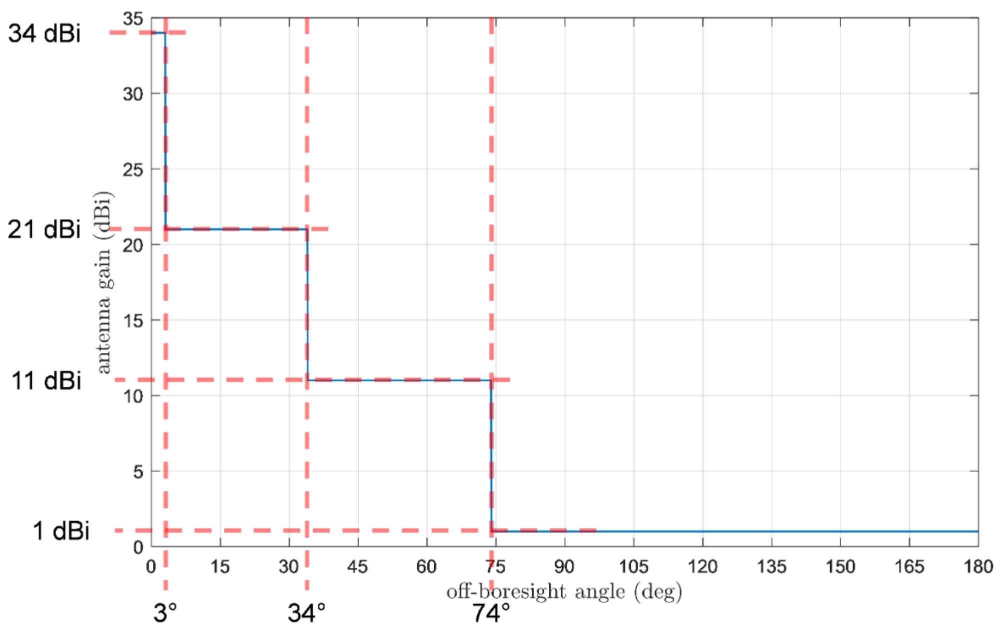

As this gain pattern is not continuous and may represent an overly pessimistic worst-case scenario, a more realistic alternative analytical model was also considered based off of Recommendation ITU-R M.1851-1.

While the antenna patterns contained in this recommendation were developed for antennas operating over the frequency band 420-33 400 MHz, they were considered here as the results should also hold over the VHF band of interest. For this analysis, the field distribution of the antenna was assumed to be uniform, leading to a sinc function type of directivity pattern, as described in equation (2) of Recommendation ITU-R M.1851-1. To make this distribution more realistic, a peak theoretical mask pattern equation was applied to the antenna gain response, as described in equation (7) of Recommendation ITU-R M.1851-1.

Specifically, if φ denotes the off-boresight angle in degrees and G_{RX} denotes the receiver antenna gain in dBi, then the following is obtained:

$$G_{RX}(\varphi) = G_{RX,\text{max}} + G_{RX,\text{rel}}(\varphi) \tag{A1-2}$$

where:

$G_{RX,\text{max}}$: main beam antenna gain in dBi

$G_{RX,\text{rel}}(\varphi)$: relative antenna gain in dB.

The relative antenna gain $G_{RX,\text{rel}}(\varphi)$ is given by equations (2) and (7) from Recommendation ITU-R M.1851-1 and yields the following here:

$$G_{RX,\text{rel}}(\varphi) = \begin{cases} 20\log\left(\left|\text{sinc}\left((l/\lambda)\sin((\pi\varphi)/180)\right)\right|\right), & 0° \le \varphi < \varphi_{\text{crit}} \\ -8.584 \cdot \ln\left(2.876 \cdot (|\varphi|/\varphi_{3\text{ dB}})\right), & \varphi_{\text{crit}} \le \varphi < 180° \end{cases} \tag{A1-3}$$

where:

l : overall length of aperture (m)

λ : wavelength (m)

φ_{crit} : critical angle peak pattern break point where mask departs from theoretical value which satisfies $G_{RX,\text{rel}}(\varphi_{\text{crit}}) = -5.75$ dB (see equation (7) in Recommendation ITU-R M.1851-1) (degree)

$\varphi_{3\text{ dB}}$: half power beamwidth, given by $\varphi_{3\text{ dB}} = 50.8(\lambda/l)$ (see equation (2) in Recommendation ITU-R M.1851-1) (degree).

For the victim receiver antenna gain pattern given by equations (A1.2) and (A1.3), the following parameters were used:

- $G_{RX,\text{max}} = 34$ dBi (using the largest value given in Recommendation ITU-R M.1226),
- $l = 56$ m (based off of an article in the literature on HyMeX described in subsequently),
- $\lambda = 6.662$ m (using a worst-case centre frequency value of 45 MHz).

From these parameter selections, the calculated quantities $\varphi_{3\text{ dB}}$ and φ_{crit} were as follows:

- $\varphi_{3\text{ dB}} = 6.043°$,
- $\varphi_{\text{crit}} = 4.106°$.

A plot of the WPR receiver antenna gain pattern using the analytical model proposed by Recommendation ITU-R M.1851-1 is given in Fig. A1-8. As can be seen, the analytical response with the peak mask pattern in play is smooth and more characteristic of an actual representative antenna pattern.

FIGURE A1-8

Nominal and peak mask appended analytical model for the victim receiver antenna gain pattern G_{RX} as a function of the off-boresight angle φ for a WPR operating near 50 MHz based off of Rec. ITU-R M.1851-1

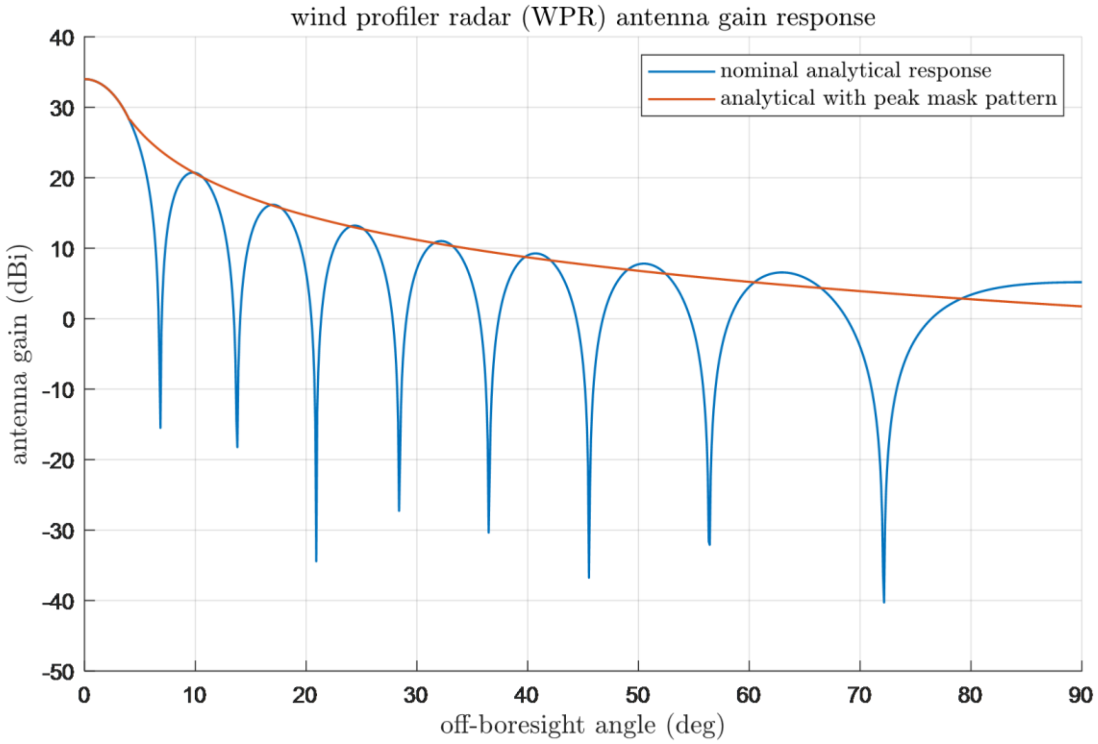

The set of fixed parameters used in the dynamic RFI simulations from the spaceborne VHF radar sounder interferer upon the candidate WPR victim is shown in Table A1-18. Here, the victim receiver bandwidth B_r was chosen to be the maximum necessary bandwidth value of 2.2 MHz.

TABLE A1-18

Parameters used in dynamic RFI simulation sharing studies to assess the impact of the spaceborne VHF radar sounder upon in-band WPR systems operating in the radiolocation service

Quantity	Units	Value
$(I/N)_{\text{IPC}}$	dB	−6
B_r	kHz	2 200
$B_{t\text{ in }r}$	kHz	2 200
NF	dB	−∞
$L_{P,\text{pol}}$	dB	0
L_{RX}	dB	0

The victim receiver antenna gain patterns considered were those derived above and shown in Figs A1-7 and A1-8. Specifically, both the pessimistic worst-case type of gain pattern (Fig. A1-7), as well as the more realistic analytical model-based gain pattern (Fig. A1-8), were considered here.

Results of dynamic RFI simulations:

The maximum received peak interference power P_r, the maximum IEL observed, and the percentage of time that the IEL exceeded 0 dB, for the WPR system radiolocation service sharing study considered here, are shown in Table A1-19. For this sharing study, the results are presented only for the most adverse WPR beam direction at zenith, and only for the rural noise environmental category.

TABLE A1-19

Maximum received peak interference power and IEL values, along with the IEL 0 dB exceedance percentage of time, for the in-band WPR radiolocation service sharing study set (assuming transmission $D_{op} \times 100\%$ = 10.79% of the time)

Environmental category	Dynamic analysis maximum received peak interference power P_r (dBW)	Dynamic analysis maximum IEL (dB)	Percentage of time IEL exceeds 0 dB (%)
Rural (Rec. ITU-R M.1226)	–53.87	70.56	0.2624
Rural (Rec. ITU-R M.1851-1)	–54.31	70.12	0.2861

Alternative calculation performed over a specific WPR location (peak power scenario)

Additional sharing studies were performed considering a specific WPR location at 68.57°S and 77.97°E (Davis, Antarctica).

The following WPR parameters were used:

– operating frequency = 55 MHz
– pulse max = 10 µs
– Antenna gain = 34 dBi
– Antenna pattern from Recommendation ITU-R F.1245
– Elevation = 90° zenith
– NF = 3 dB
– BW = 2.2 MHz
– kTBF = −137.55 dBW
– Environnement (rural) external noise = −181.85 dBW/Hz
– TOTAL NOISE = −118.4 dBW
– *I/N* = −6 dB
– Ionospheric attenuation = 2.3 dB
– OTR calculated based on equation 4a of Recommendation ITU-R RS.1260

$$OTR = 10 \log\left(\frac{B_r^2 \tau}{B_c}\right) \quad \text{for} \quad \frac{B_r^2 \tau}{B_c} < 1$$

where:

B_r: other service receiver IF bandwidth

B_c: chirp bandwidth of spaceborne sensor

τ: sensor pulse width.

In-band scenario

When considering peak interference for the in-band scenario (40-50 MHz), calculations lead to the following interference distributions:

FIGURE A1-9

Interference distribution over a specific WPR location in Antarctica

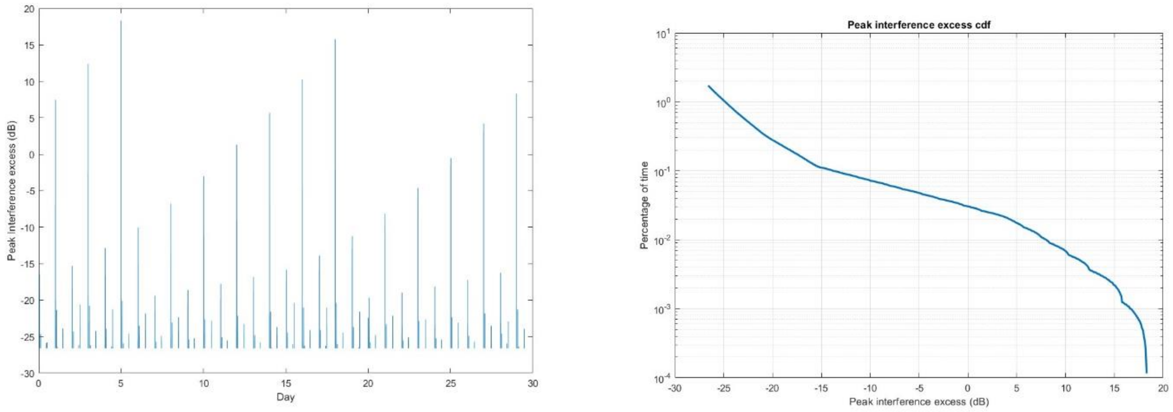

The WPR protection criteria (−6 dB *I*/*N*) is potentially exceeded for 0.027% of the time. The maximum exceedance is of 18 dB.

Adjacent band scenario

As most of WPR around 50 MHz, the WPR under study is operated at 55 MHz, i.e. out-of-band from EESS (active) sensor.

The typical wave form of EESS sensor is depicted in Fig. 5.

At 55 MHz, the attenuation is about 60 dB, meaning that in adjacent band situation, there will be no interference from EESS (active) to Wind profiler radars.

Additional considerations related to WPR deployment

Due to the objectives of the spaceborne radar sounder (to understand the global thickness, inner structure, and the thermal stability of the Earth's ice sheets (e.g. in Greenland and Antarctica)) as an observable parameter of Earth's climate evolution, the small number of existing WPRs operating in the 40-50 MHz and the opportunity for further WPRs to be deployed above 50 MHz in the future, it is considered that, based on the above elements in addition to the results of the completed studies, coordination on a case by case basis with the spaceborne radar sounder could be performed to ensure the protection of WPR operating in the 40-50 MHz frequency range.

A1.3.2 Space research service sharing studies

As with the fixed service sharing studies, over the 40-50 MHz VHF band of interest, there are no technical characteristics for systems operating in the space research service in the ITU-R Recommendations. Because of this, a nominal set of parameters was used for the dynamic RFI simulations. Specifically, no internal noise source was considered, there was no gain or attenuation assumed for the receiver antenna, and no losses were attributed to polarization mismatch or receiver hardware effects. Based on these assumptions and the data from Table 3, the relevant quantities used for the space research service sharing studies are given in Table A1-20.

TABLE A1-20

Parameters used in dynamic RFI simulation sharing studies to assess the impact of the spaceborne VHF radar sounder upon the in-band space research service

Quantity	Units	Value
$(I/N)_{\text{IPC}}$	dB	−6
B_r	kHz	1
$B_{t\text{ in }r}$	kHz	1
NF	dB	0
G_{RX}	dBi	0
$L_{P,\text{pol}}$	dB	0
L_{RX}	dB	0

The maximum received peak interference power P_r, the maximum IEL observed, and the percentage of time that the IEL exceeded 0 dB, for each noise environmental category for the space research service sharing study, are shown in Table A1-21.

TABLE A1-21

Maximum received peak interference power and IEL values, along with the IEL 0 dB exceedance percentage of time, for the in-band space research service sharing study set (assuming transmission $D_{op} \times 100\%$ = 10.79% of the time)

Environmental category	Dynamic analysis maximum received peak interference power P_r (dBW)	Dynamic analysis maximum IEL (dB)	Percentage of time IEL exceeds 0 dB (%)
City	−138.50 (Ghardaïa) −138.81 (Alert)	10.38 (Ghardaïa) 10.08 (Alert)	0.0058 (Ghardaïa) 0.0765 (Alert)
Residential		14.54 (Ghardaïa) 14.24 (Alert)	0.0098 (Ghardaïa) 0.1109 (Alert)
Rural		19.34 (Ghardaïa) 19.04 (Alert)	0.0165 (Ghardaïa) 0.1618 (Alert)

It should be noted that no use of the SRS allocation at 40 MHz has been reported during the development of this Report.

A1.4 Selected out-of-band dynamic analysis based sharing studies

The methods used to calculate the IEL discussed in § 4 technically only apply for the case in which the victim receiver BW lies entirely within the interferer transmitter BW. This assumption manifests itself in the form of the FDR from equation (8), and the OTR from equation (9).

For the more general case, in which there are no assumptions regarding the relative positions of the interferer transmitter power spectrum and victim receiver filter, the peak interference power P_r from Equation (3) is computed via the following formula:

$$P_r = P_{r,\text{nom}} + G_{TX} + G_{RX} - L_{TX} - L_P - L_{RX} \tag{A1-4}$$

where:

P_r : peak received interference power (dBW)
$P_{r,\text{nom}}$: nominal peak received interference power (dBW)
G_{TX} : transmitter antenna gain (dBi)
G_{RX} : receiver antenna gain (dBi)
L_{TX} : transmit feeder and associated losses (feeder, connectors, etc.) (dB)
L_P : propagation path loss between transmitting and receiving antennas (dB)
L_{RX} : receiver feeder and associated losses (feeder, connectors, etc.) (dB).

The nominal received interference power $P_{r,\text{nom}}$ from equation (A1-4) is calculated by passing the interferer transmitted PSD $S_{TX}(f)$ through the victim receiver filter frequency response $H_{RX}(f)$:

$$P_{r,\text{nom}} = 10\log\left(\int_{-\infty}^{\infty} |H_{RX}(f)|^2 S_{TX}(f)\, df\right) \tag{A1-5}$$

where:

$P_{r,\text{nom}}$: nominal peak received interference power (dBW)
$S_{TX}(f)$: interferer transmitted PSD (W/MHz)
$H_{RX}(f)$: victim receiver filter frequency response
f : frequency (MHz).

For this analysis, the interferer transmitted PSD $S_{TX}(f)$ from equation (A1-5) can be the emission spectrum shown in Fig. 5. In addition, for the out-of-band sharing studies, the victim receiver filter frequency response $H_{RX}(f)$ can be approximated as a constant in the passband and zero outside of this region. Under these assumptions, the nominal received interference power $P_{r,\text{nom}}$ from equation (A1-5) can be approximated to the following expression.

$$P_{r,\text{nom}} \approx P_{TX} - 10\log(B_t) + 10\log(B_r) - 30 - A \tag{A1-6}$$

where:

$P_{r,\text{nom}}$: nominal peak received interference power (dBW)
P_{TX} : peak transmitter output power (dBW)
B_t : transmitter 3 dB bandwidth (MHz)
B_r : receiver 3 dB bandwidth (kHz)
A : attenuation factor (dB).

Here, the attenuation factor A represents the amount of attenuation of the interferer transmitted PSD $S_{TX}(f)$ from its average in-band value to its value in the victim receiver band of interest. For example, from the emission spectrum shown in Fig. 5, the attenuation factor just outside of the 40-50 MHz frequency range is about 20 dB and quickly grows to about 60 dB around 5 MHz away from the 40-50 MHz band.

Combining equation (A1-6) with equation (A1-4) and equation (2), the following approximation for the observed interference PSD I is obtained:

$$I = P_{TX} - 10\log(B_t) - 60 - A + G_{TX} + G_{RX} - L_{TX} - L_P - L_{RX} \tag{A1-7}$$

where:

I : observed interference PSD (dBW/Hz)
P_{TX} : peak transmitter output power (dBW)
B_t : transmitter 3 dB bandwidth (MHz)
A : attenuation factor (dB)
G_{TX} : transmitter antenna gain (dBi)
G_{RX} : receiver antenna gain (dBi)
L_{TX} : transmit feeder and associated losses (feeder, connectors, etc.) (dB)
L_P : propagation path loss between transmitting and receiving antennas (dB)
L_{RX} : receiver feeder and associated losses (feeder, connectors, etc.) (dB).

For the out-of-band sharing studies, the IEL is calculated as before, but with the peak received power P_r calculated using equation (A1-4), using the approximation of the nominal value $P_{r,\text{nom}}$ given in equation (A1-6). Equivalently, the observed interference PSD I is computed using equation (A1-7) and then the IEL is calculated via equation (1).

A1.4.1 Amateur service (50-54 MHz) dynamic analysis based sharing studies

Parameters for systems operating in the amateur service in the 50-54 MHz frequency band can be found in Tables 1A, 2A and 3A of Recommendation ITU-R M.1732-2 and Table 9 of Report ITU-R M.2478. Using selected parameters from these tables in a dynamic RFI analysis with respect to the spaceborne VHF radar sounder, similar in setup to that described in § A1.2, leads to the values found in Table A1-22.

TABLE A1-22

Parameters used in dynamic RFI simulation sharing studies to assess the impact of the spaceborne VHF radar sounder upon the adjacent out-of-band (50-54 MHz) amateur service

Quantity	Units	Value
$(I/N)_{\text{IPC}}$	dB	–6
A	dB	20
G_{RX}	half-wave dipole (equation (5)), tilt angles β of 5° and 10°	
$L_{P,\text{pol}}$	dB	3
L_{RX}	dB	1
NF	dB	0.5

Here, the attenuation was selected to be 20 dB, which matches the value at the band edge of 50 MHz (see Fig. 5). This very conservative value was chosen as there may be amateur services operating very close to the 50 MHz lower band edge. Specifically, 24/7 propagation beacons along with narrowband weak-signal communications, such as continuous wave (CW), single-sideband (SSB), and digital weak signal data modes, may occupy the 50.0-50.5 MHz band, as shown in Table A1-1 of Report ITU-R M.2478. For the victim receiver antenna gain G_{RX}, a half-wave dipole response from Equation (5), for which the maximum gain is 2.15 dBi, was used to closely match the 2.5 dBi omnidirectional value from Table 9 of Report ITU-R M.2478. In addition, the polarization loss $L_{P,\text{pol}}$ was set to 3 dB to account for the mismatch between the spaceborne VHF radar sounder circular polarization (see Table 1) and either the horizontal or vertical polarizations for the amateur service systems given in Tables 1A, 2A and 3A of Recommendation ITU-R M.1732-2. Finally, the receiver loss factor L_{RX} was set to 1 dB and the noise figure NF was set to 0.5 dB to match the minimum feeder loss and receiver noise figure values for the 50-54 MHz amateur service systems characterized in Tables 1A, 2A, and 3A of Recommendation ITU-R M.1732-2.

The maximum received peak interference power P_r, the maximum IEL observed, and the percentage of time that the IEL exceeded 0 dB, for each noise environmental category for the amateur service sharing study, are shown in Table A1-23.

TABLE A1-23

Maximum received peak interference power and IEL values, along with the IEL 0 dB exceedance percentage of time, for the adjacent out-of-band (50-54 MHz) amateur service sharing study set (assuming transmission $D_{op} \times 100\%$ = 10.79% of the time)

Environmental category	Receiver antenna tilt angle (degrees)	Dynamic analysis maximum received peak interference power P_r (dBW)	Dynamic analysis maximum IEL (dB)	Percentage of time IEL exceeds 0 dB (%)
City	5	−148.14 (Ghardaïa) −148.44 (Alert)	−11.29 (Ghardaïa) −11.60 (Alert)	0 (Ghardaïa) 0 (Alert)
Residential	5		−7.13 (Ghardaïa) −7.44 (Alert)	0 (Ghardaïa) 0 (Alert)
Rural	5		−2.33 (Ghardaïa) −2.64 (Alert)	0 (Ghardaïa) 0 (Alert)
City	10	−146.68 (Ghardaïa) −147.00 (Alert)	−9.85 (Ghardaïa) −10.16 (Alert)	0 (Ghardaïa) 0 (Alert)
Residential	10		−5.69 (Ghardaïa) −6.00 (Alert)	0 (Ghardaïa) 0 (Alert)
Rural	10		−0.88 (Ghardaïa) −1.19 (Alert)	0 (Ghardaïa) 0 (Alert)

A1.5 Complementary cumulative distribution function profiles of the interference exceedance level

To expand upon the static analysis considered in § A1.1, dynamic simulations were carried out as explained in the previous sections (§§ A1.2, A1.3 and A1.4). From these, complementary cumulative distribution function (CCDF) curves of the IEL, shown below in Figs A1-10, A1-11, A1-12 and A1-13, were generated to qualitatively understand the amount of time the radar sounder violates the IPC limits for each incumbent radio service. For the generic systems for which no receiver antenna gain pattern was available, namely the systems considered in Figs A1-10, A1-11, A1-12 and A1-13, a half-wave dipole receiver antenna with gain as in equation (5) with a tilt angle β of 5° was used.

In addition, for all cases considered in Figs A1-10, A1-11, A1-12 and A1-13, the CCDF curves account for the maximum fractional amount of time that the radar sounder will be operational. Namely, recall from §§ 2.4 and 3.4 of Recommendation ITU-R RS.2042 that the sounding radar will operate for a period not to exceed 10 minutes in duration per 92.7 minute orbit.

As such, the fraction of time over which the radar sounder will be operational is at most $D_{op} = 10/92.7 \approx 0.1079$, a quantity referred to as the operational duty cycle (not to be confused with the signal waveform duty cycle). It should be noted that the operational duty cycle here represents an upper bound on the fraction of time that the sounder will be operating. In practice, when illuminating over a specific geographical location, the total amount of time the sounder will be emitting will be conditional with respect to this operational duty cycle. To model this upper bound on the fraction of time the sounder will be transmitting, the operational duty cycle was factored into the dynamic simulations and the CCDF curves from Figs A1-10, A1-11, A1-12 and A1-13 account for this phenomenon.

Furthermore, in Figs A1-10, A1-11, A1-12 and A1-13, a rural noise environment was considered. While results were generated for the city and residential noise environmental categories and are stated elsewhere in this Report, the rural results were plotted here as these represent the most adverse set of operating conditions for the spaceborne VHF radar sounder in terms of interference to victim services.

FIGURE A1-10

Empirical CCDF plots of the IEL from the spaceborne VHF radar sounder to in-band primary/secondary services with generic receiver systems (fixed, mobile, broadcasting, radiolocation, and space research), in a rural noise environment (a half-wave dipole antenna gain pattern from equation (5) was used along with a tilt angle β of 5°)

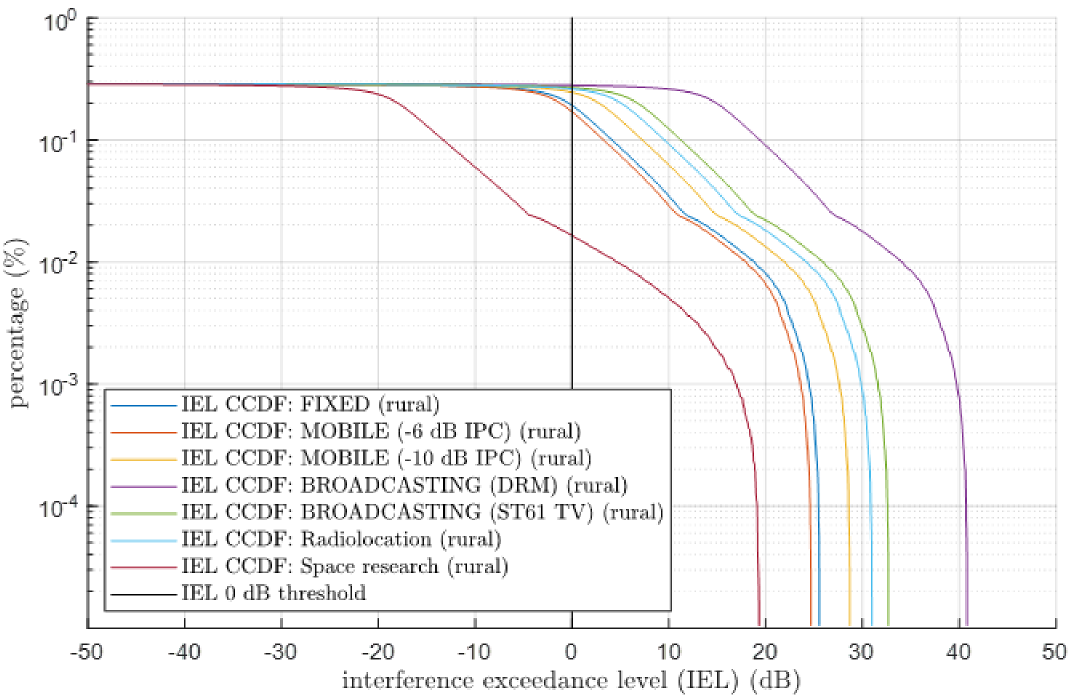

FIGURE A1-11

Empirical CCDF plots of the IEL from the spaceborne VHF radar sounder to the oceanographic radar (OR) systems considered in § A1.3.1.1, in a rural noise environment

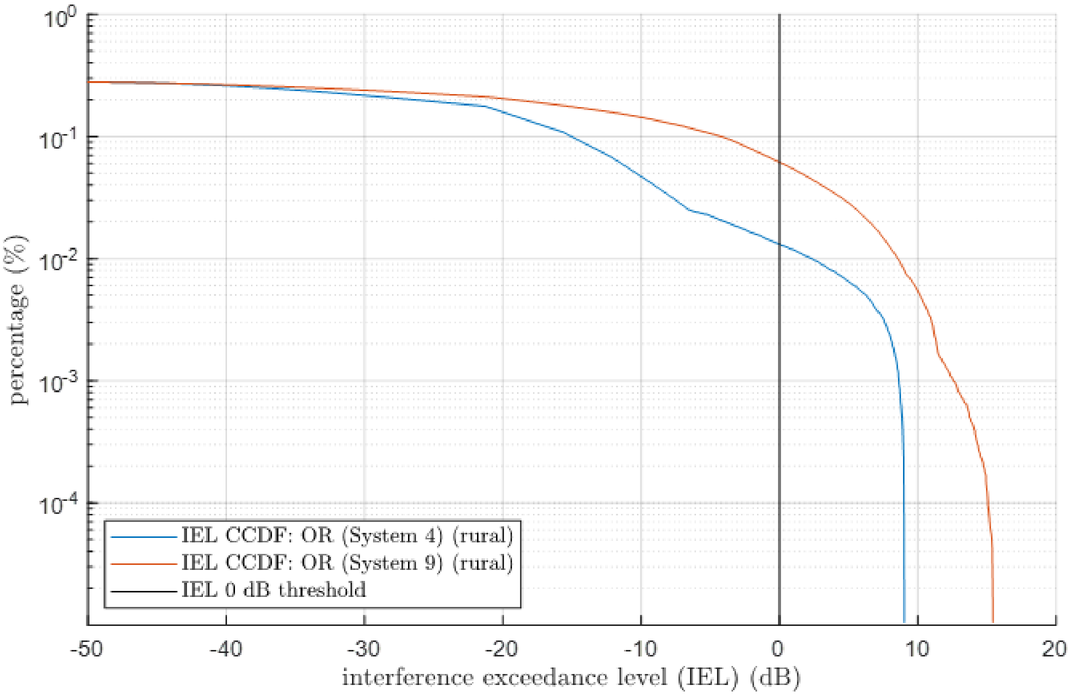

FIGURE A1-12

Empirical CCDF plots of the IEL from the spaceborne VHF radar sounder to the wind profiler radar (WPR) systems considered in § A1.3.1.2, in a rural noise environment

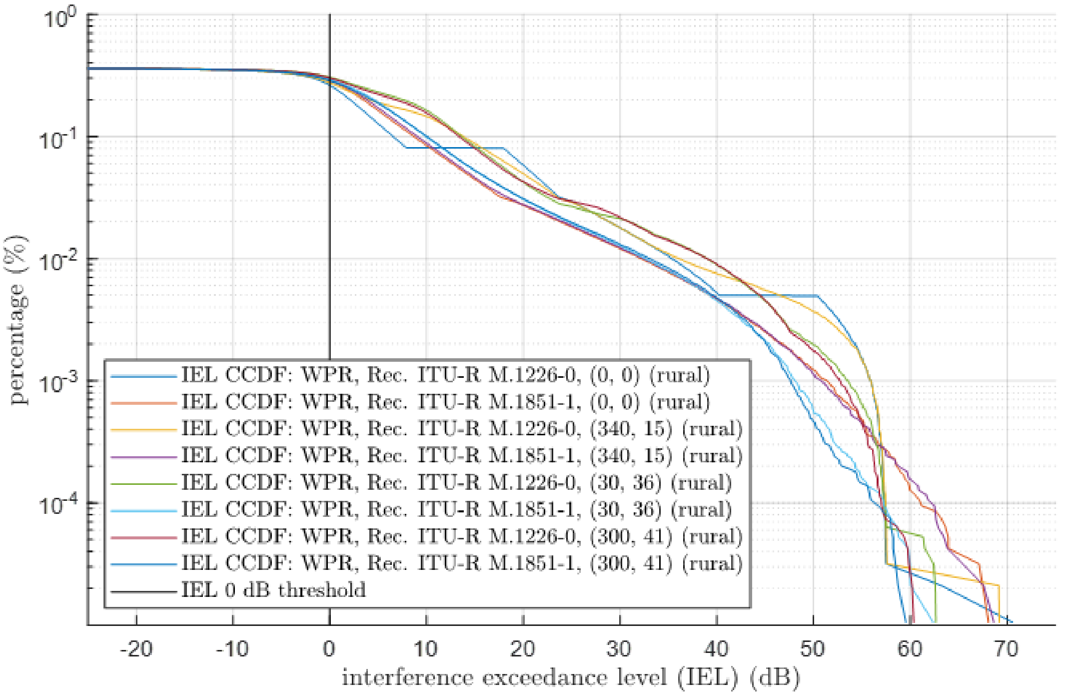

FIGURE A1.13

Empirical CCDF plots of the IEL from the spaceborne VHF radar sounder to the adjacent out-of-band (50-54 MHz) amateur service considered in § A1.4.1, in a rural noise environment (a half-wave dipole antenna gain pattern from equation (5) was used along with a tilt angle β of 5°)

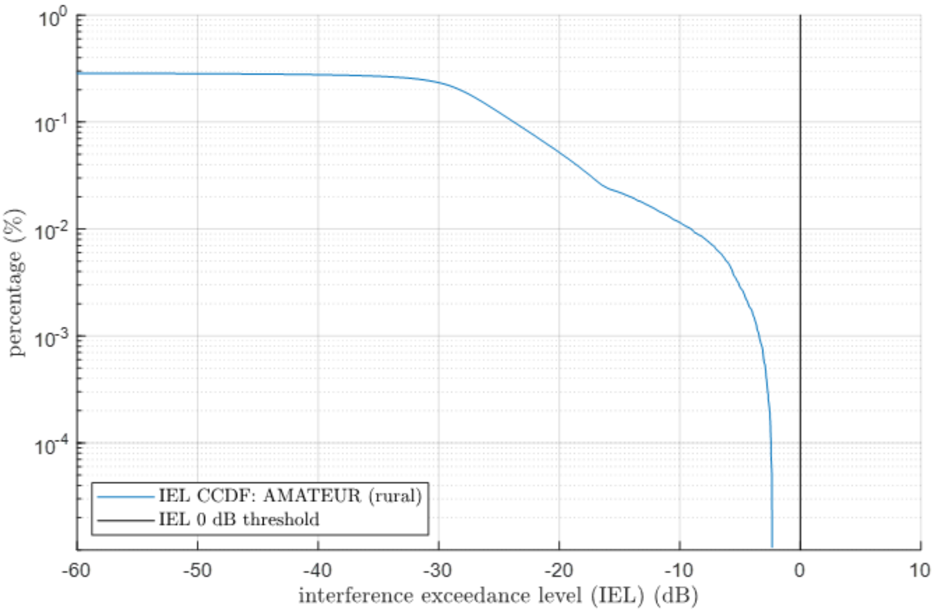

The percentage of time that the IEL breached the 0 dB IPC target limit is given in Tables A1-5, A1-7, A1-9, A1-11, A1-15, A1-19, A1-21 and A1-23 for all of the victim services and noise environmental categories considered in this Report. From these tables, it can be seen that in the worst cases, the percentage of time over the course of the observation epoch for which an IEL target limit of 0 dB was violated was on the order of 0.3% of the time for the victim sites at Ghardaïa, Tripoli, and Pianottoli, and was on the order of 1.5% of the time for the victim site at Alert.

Annex 2

Sharing and compatibility studies using the mean power based interference analysis

In Annex 1 of this Report, the sharing studies considered the peak interference power P_r, calculated as shown in equation (3), in order to determine the observed interference-to-noise PSD $(I/N)_{\text{obs}}$ using equation (2), and subsequently the IEL as shown in equation (1).

However, this metric may not be a realistic reflection of the actual interference received by a victim incumbent service system. Specifically, as the spaceborne VHF radar sounder is a pulsed radar system, the interference power from such a system only achieves its peak value while the radar pulse is active, and is ideally zero or practically close to zero when the radar pulse is inactive. To address this phenomenon, a more relevant metric to assess the level of interference from the spaceborne VHF radar sounder would be the mean or average interference power, which simultaneously accounts for both the active and inactive phases of the radar pulse.

For a pulsed radar system, the mean power can be calculated from the peak power by applying a factor equal to the fraction of time that the pulse is active, called the duty cycle, which is the product of the pulse repetition frequency (PRF) with the pulsewidth. Specifically, the mean interference power P_{r_mean} can be computed from the peak interference power P_r via equation (4):

Using P_{r_mean} in place of P_r to compute the observed interference-to-noise PSD $(I/N)_{\text{obs}}$ as in equation (2), and using this value in turn in equation (1), results in an IEL calculated according to the mean interference power, which is denoted here as IEL_{mean}.

From Table 1, it can be seen that $PRF = 1\,200$ Hz and $\tau = 85$ µs.

From Table 3 of Recommendation ITU-R P.531, the magnitude of the ionospheric absorption loss at mid-latitude is equal to $loss$ = 0.01 dB at a frequency f=1GHz. This corresponds to the fraction of total electron content (TEC) of the ionosphere seen at the altitude of the propagation path equal to $TEC = 1$, $f = 1$ GHz and the constant of proportionality of $C = 8660.254$. By transposing to $f =$ 45 MHz and considering $TEC = 0.54$ (as determined in a previous study, see Report ITU-R RS. 2455-0) then the propagation losses due to atmospheric effects have been determined as $loss = \frac{C*TEC}{f(MHz)^2}$ and would give 2.3 dB. This factor of 2.3 dB has been consider in the studies in Annex 2 as the miscellaneous propagation path loss factor given in equation (6) of the Report.

A2.1 Complementary cumulative distribution function profiles of the interference exceedance level

Employing the mean power based IEL metric IEL_{mean} in place of the nominal IEL for the CCDF based statistical analysis leads to the percentage of time that the respective IEL violated the 0 dB IPC target limit for each victim scenario shown in Table A2-1.

TABLE A2-1

Empirical CCDF derived values for mean power based IEL for the victim scenarios considered in this sharing and compatibility study

Victim scenario description	Percentage of time mean power based IEL breached 0 dB IPC target limit (%)	Mean power based IEL (dB)	Corresponding elevation angle δ for mean power based IEL (degrees)
FIXED (city)	0.0017	0.7249	74.2342
FIXED (residential)	0.0074	4.8790	59.6396
FIXED (rural)	0.0156	9.6654	50
MOBILE (–6 dB *I*/*N* IPC) (city)	0.0004	−0.1324	83.4234
MOBILE (–6 dB *I*/*N* IPC) (residential)	0.0062	4.0100	61.8919
MOBILE (–6 dB *I*/*N* IPC) (rural)	0.0143	8.6	50
MOBILE (–10 dB *I*/*N* IPC) (city)	0.006	3.8676	62.2523
MOBILE (–10 dB *I*/*N* IPC) (residential)	0.0131	8.0100	52.9730
MOBILE (–10 dB *I*/*N* IPC) (rural)	0.0226	12.7582	45.1351

TABLE A2-1 *(cont.)*

Victim scenario description	Percentage of time mean power based IEL breached 0 dB IPC target limit (%)	Mean power based IEL (dB)	Corresponding elevation angle δ for mean power based IEL (degrees)
BROADCASTING (DRM, G_{RX} = 2.15 dBi) (city)	0.0258	13.8749	43.5135
BROADCASTING (DRM, G_{RX} = 2.15 dBi) (residential)	0.0384	18.0290	38.2883
BROADCASTING (DRM, G_{RX} = 2.15 dBi) (rural)	0.0510	22.8154	34.7748
BROADCASTING (DRM, G_{RX} = −0.05 dBi) (city)	0.0201	11.6749	46.7568
BROADCASTING (DRM, G_{RX} = −0.05 dBi) (residential)	0.0312	15.8290	40.9910
BROADCASTING (DRM, G_{RX} = −0.05 dBi) (rural)	0.0484	20.6154	35.4054
BROADCASTING (DRM, G_{RX} = −20.61 dBi) (city)	–	–	83.4234
BROADCASTING (DRM, G_{RX} = −20.61 dBi) (residential)	–	–	83.4234
BROADCASTING (DRM, G_{RX} = −20.61 dBi) (rural)	0.00035	–	80.9009
BROADCASTING (ST61 TV, G_{RX} = 0.15 dBi) (city)	0.0206	11.8749	46.4865
BROADCASTING (ST61 TV, G_{RX} = 0.15 dBi) (residential)	0.0320	16.0290	40.7207
BROADCASTING (ST61 TV, G_{RX} = 0.15 dBi) (rural)	0.0510	20.8154	35.1351
Radiolocation (city)	0.0017	0.7249	74.2342
Radiolocation (residential)	0.0074	4.8790	59.6396
Radiolocation (rural)	0.0156	9.6654	50
Space research (city)	0	–	–
Space research (residential)	0	-	–
Space research (rural)	0	–	–
Oceanographic radar (System 4) (city)	0.0017	–	–

TABLE A2-1 *(end)*

Victim scenario description	**Percentage of time mean power based IEL breached 0 dB IPC target limit (%)**	**Mean power based IEL (dB)**	**Corresponding elevation angle δ for mean power based IEL (degrees)**
Oceanographic radar (System 4) (residential)	0.0076	1.9259	58.4685
Oceanographic radar (System 4) (rural)	0.0167	6.4030	57.7568
Oceanographic radar (System 9) (city)	0.0116	4.63	72.6126
Oceanographic radar (System 9) (residential)	0.0269	8.7509	73.7838
Oceanographic radar (System 9) (rural)	0.0510	13.4549	72.3423
WPR, Rec. ITU-R M.1226, (0°, 0°) (city) (in-band)	0.0916	59.6156	27.7477
WPR, Rec. ITU-R M.1226, (0°, 0°) (residential) (in-band)	0.1550	63.7697	22.1622
WPR, Rec. ITU-R M.1226, (0°, 0°) (rural) (in-band)	0.2002	68.5561	16.3063
WPR, Rec. ITU-R M.1851, (0°, 0°) (city) (in-band)	0.0510	59.6131	34.6847
WPR, Rec. ITU-R M.1851, (0°, 0°) (residential) (in-band)	0.0745	63.7672	30.0901
WPR, Rec. ITU-R M.1851, (0°, 0°) (rural) (in-band)	0.1227	68.5536	24.5946
AMATEUR (city) (adjacent-band)	–	–	–
AMATEUR (residential) (adjacent-band)	–	–	–
AMATEUR (rural) (adjacent-band)	–	–	–

As stated in § 2.4, the spaceborne radar sounders will operate approximately 10 minutes per orbit (each orbit lasts 92.7 minutes). Also, the times of operation of the spaceborne radar sounders are likely to be focused in the areas highlighted in § 2.4. This is why, for the calculation of the mean IEL, it was considered that the radar sounder only works in the morning as it is specified in § 2.4 so the visibility blocks in the afternoon will be without emissions as it will be seen below.

A2.2 Analysis of the temporal interference from EESS (active) into the mobile service

An example was taken using the mobile service for an $I/N = -6$ dB with a station located at Vilnius:

Latitude: 56.23270°N,

Longitude: 25.49110°E,

Altitude: 10 m.

Using the same setup described in § 5, a set of dynamic RFI simulations were carried out, in which the spaceborne VHF radar sounder was considered. In order to represent a typical operational scenario for the sounder, each dynamic simulation was carried out over a 12-day period, with the relevant RFI metrics being calculated at 1 s increments. The specific observation epoch start time considered for this set of analyses was 2015/07/29 10:00:00 UTC.

The results of these simulations are provided below in Fig. A2-1, providing the timeline (over 12 days) of the elevation to which the satellite is seen from the mobile station location and Fig. A2-2 giving the duration of the corresponding events.

In addition, since the VHF radar sounder will only transmit in the morning (around 4 AM), the visibility blocks in the afternoon will be without emissions as it will be seen below. It means that only can considered the morning blocks (orange blocks) and only the elevations above 50 degrees (elevation angle from where the interference starts for the dipole, see Table A2-1).

FIGURE A2-1

Station in Vilnius: elevations of the satellite for a period of 12 days

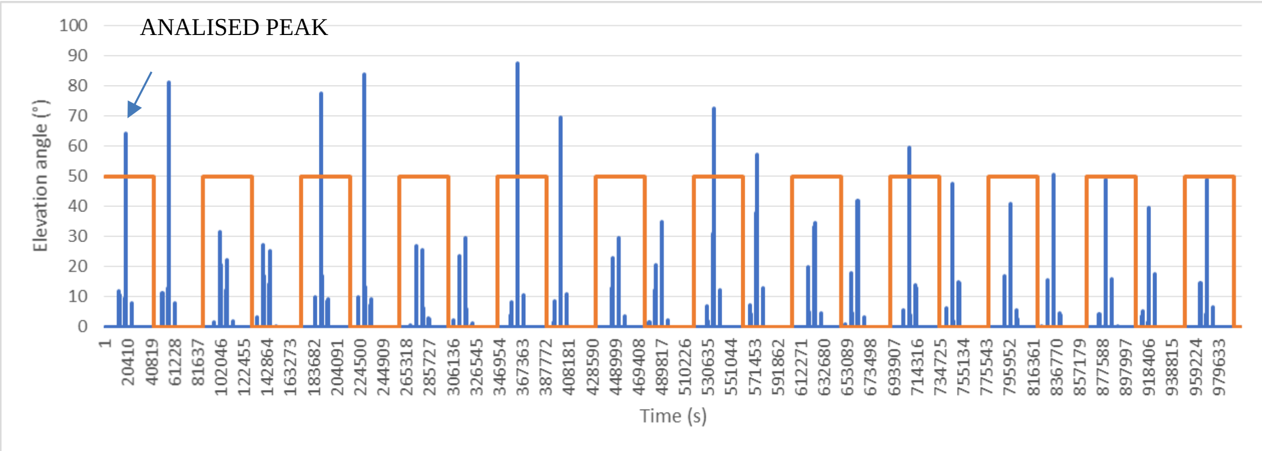

FIGURE A2-2

Station in Vilnius: time of exceedance of protection criteria for 12 days

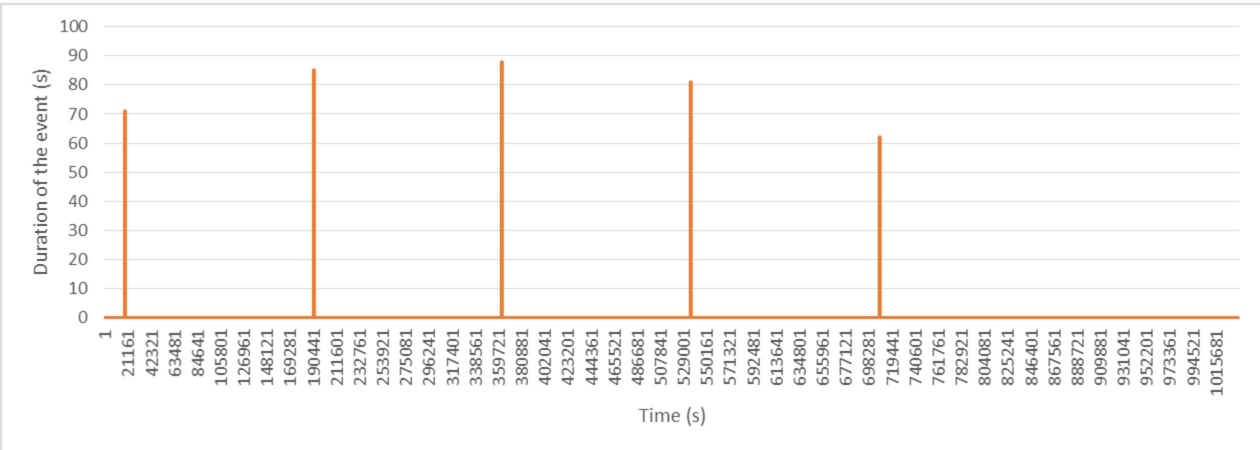

Globally, over the 12 days, there are only five periods of time of exceedance with maximum durations of 60 to 90s, representing in total 0.037% of time.

Finally, it is also interesting to make a detailed analysis of these exceedance events. Figure A2-3 is a zoom over the first peak. (actually, with the precise values of *I*/*N* vs Elevation, it is possible to refine the actual length of interference from 70 s to 64 s).

FIGURE A2-3

Station in Vilnius: time of exceedance of protection criteria for the analysed peak specified in Fig. A2-1

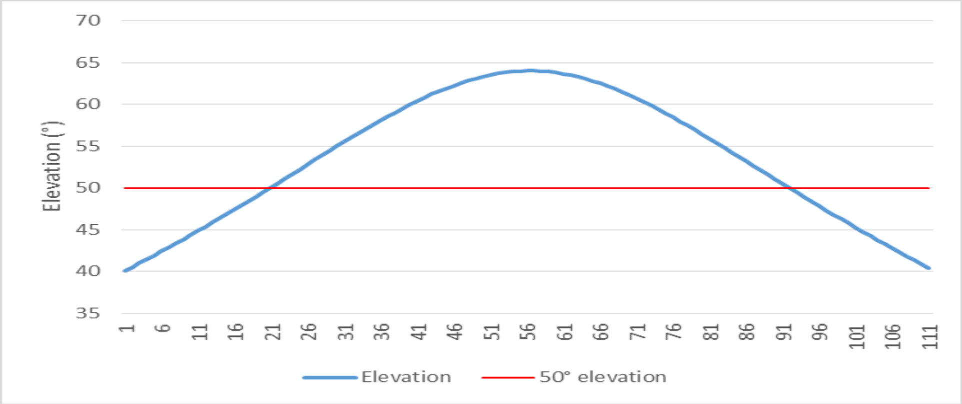

Over the same period of time, using the elevation above and the corresponding *I*/*N* value as in Fig. A2-3, it is possible to determine curves of protection criteria exceedance (red curve in Fig. A2-4).

FIGURE A2-4

Station in Vilnius: Exceedance of criteria and the corresponding *I*/*N*

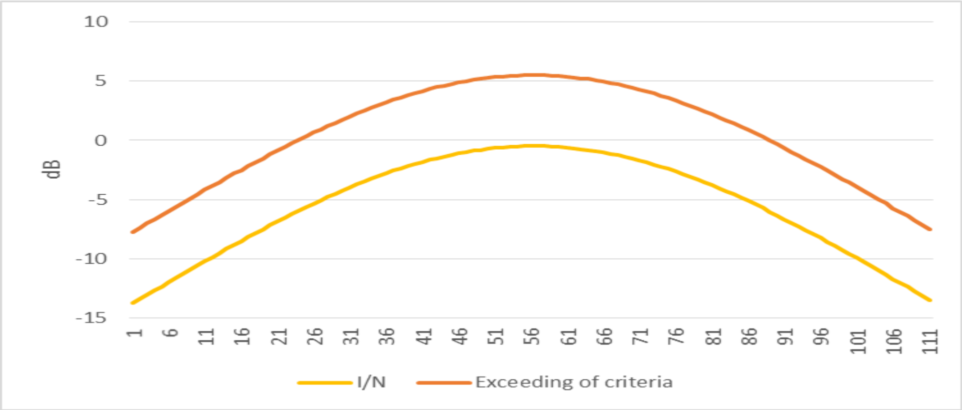

Finally, recognising that *I*/*N* values can be turned into margin degradation, the following Fig. A2-5 provides the corresponding mobile service station margin degradation (blue curve in Fig. A2.5) but also the additional margin degradation compared to the one corresponding to an *I*/*N* of −6 dB (green curve in Fig. A2-5).

FIGURE A2-5

Station in Vilnius: Margin degradation and additional margin degradation compared to *I/N* = −6 dB

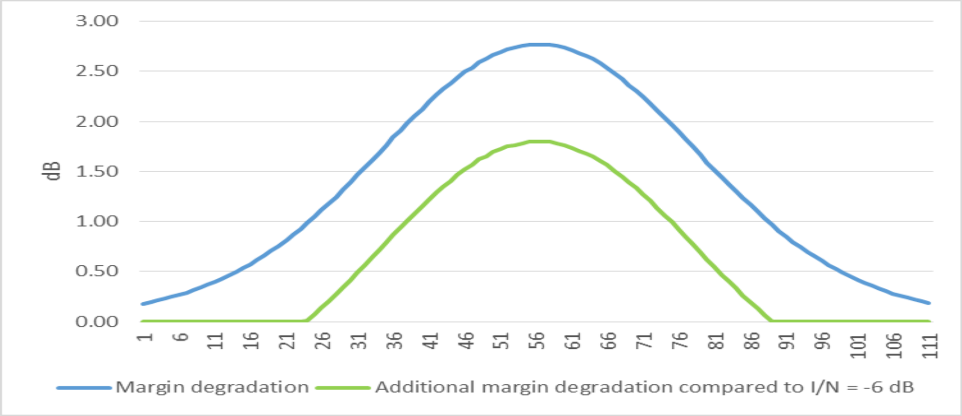

In Fig. A2-5 it can be seen that for these interference events, the worse-case margin degradation will be of less than 3 dB (calculated considering the maximum of 8.6 dB exceedance as given in Table A2-1 where *I*/*N* of −6 dB was removed) and less than 2 dB compared to what is already acceptable with an *I*/*N* = −6 dB for this specific studied peak.

A2.3 Alternative calculation on the interference from EESS (active) into WPR performed over a specific WPR location (mean power scenario)

Additional sharing studies were performed considering a specific WPR location at 68.57°S and 77.97°E (Davis, Antarctica).

The following WPR parameters were used:

– operating frequency = 55 MHz
– Antenna gain = 34 dBi
– Antenna pattern from Recommendation ITU-R F.1245
– Elevation = 90° zenith
– NF = 3 dB
– BW = 2.2 MHz
– kTBF = −137.55 dBW
– Environnement (rural) external noise = −181.85 dBW/Hz
– TOTAL NOISE = −118.4 dBW
– *I/N* = −6 dB
– Ionospheric attenuation = 2.3 dB
– OTR calculated based on equation 2a of Recommendation ITU-R RS.1260

$$OTR = 10 \log (B_r / B_t) \text{ for } B_r \leq B_t$$

where:

B_r: receiver bandwidth

B_t: bandwidth of the transmitted interfering signal.

In-band scenario

When considering mean interference for the in-band scenario (40-50 MHz), calculations lead to the following interference distributions:

FIGURE A2-6

Interference distribution over a specific WPR location in Antarctica

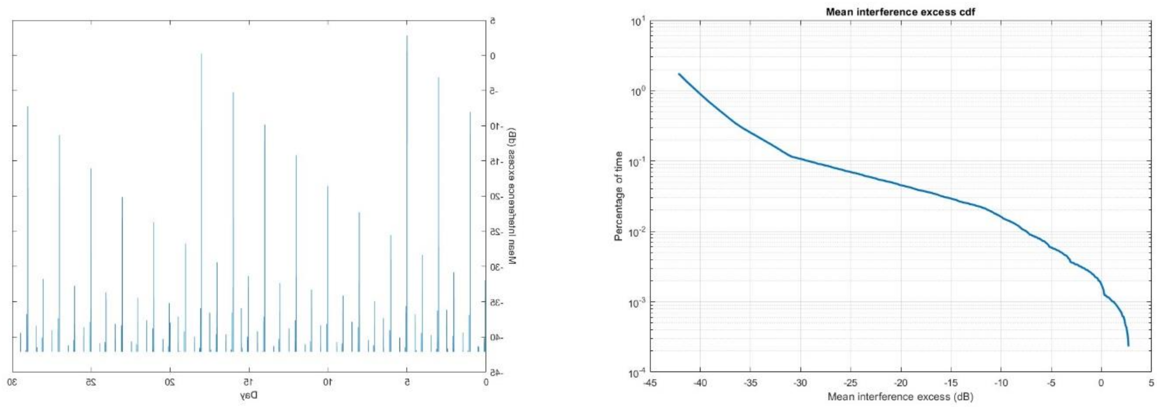

The WPR protection criteria (−6 dB I/N) is potentially exceeded for 0.0008% of the time. The Maximum exceedance is of 2 dB.

Adjacent band scenario

As most of WPR around 50 MHz, the WPR under study is operated at 55 MHz, i.e. out-of-band from EESS (active) sensor.

The typical wave form of EESS sensor is depicted in Fig. 5.

At 55 MHz, the attenuation is about 60 dB, meaning that in adjacent band situation, there will be no interference from EESS (active) to wind profiler radars.

Annex 3

Determination of the pfd of the spaceborne radar sounder and the pfd for the protection of incumbent services

A3.1 Power flux-density of the spaceborne radar sounder considered in the Report

Using the formula for the pfd given in No. **21.16.8** of the RR Articles, Edition of 2020 for the mean pfd value, the mean pfd value is obtained by the following expression:

$$PFD(\delta) = P_{TX} + 10\log(PRF) + 10\log(\tau) - 10\log(B_t) + 10\log(B_{\text{ref}}) + G_{TX}\big(\theta(\delta)\big)$$
$$-10\log\left(4\pi\big(d(\delta)\big)^2\right) - 150 \quad \text{(A3-1)}$$

where:

- PFD : power flux-density (dB(W/m^2)) in the reference bandwidth
- δ : elevation angle from the victim location to the interferer position (degree)
- P_{TX} : peak transmitter output power (dBW)
- PRF : pulse repetition frequency (Hz)
- τ : pulsewidth (µs)
- B_t : transmitter 3 dB bandwidth (MHz)

B_{ref} : reference bandwidth (kHz)

G_{TX} : transmitter antenna gain (dBi)

θ : separation angle from the interferer boresight to the victim location (degree)

d : distance between the interferer and victim (km).

Assuming that the spaceborne VHF radar sounder interferer is at a constant altitude with respect to the victim, the separation angle θ as a function of the elevation angle δ is given by the law of sines to be the following:

$$\theta(\delta) = \frac{180°}{\pi} \arcsin\left[\left(\frac{R_E}{R_E+h}\right)\cos\left(\frac{\pi}{180°}\delta\right)\right] \quad \text{(A3-2)}$$

where:

R_E : radius of the Earth value of 6 378.137 km (km)

h : altitude of interferer (km).

From the expression for the separation angle $\theta(\delta)$ given in equation (A3-2), the distance d between the interferer and victim as a function of the elevation angle δ from equation (A3-1) is given by the following formula after some trigonometric manipulation:

$$d(\delta) = (R_E + h)\cos\left[\frac{\pi}{180°}\theta(\delta)\right] - R_E \sin\left(\frac{\pi}{180°}\delta\right) \quad \text{(A3-3)}$$

Combining equations (A3-2) and (A3-3) into equation (A3-1), the pfd as a function of the elevation angle δ is obtained. Using the design parameters for the spaceborne VHF radar sounder given in § 2.2, a plot of the pfd as a function of the elevation angle is given in Fig. A3-1, for a reference bandwidth of 4 kHz.

Similarly, the peak pfd value can be calculated by removing the signal duty cycle factor from the formula used to calculate the mean pfd value.

From Fig. A3-1, the maximum mean pfd value is −135.96 dB(W/m^2 4 kHz) and the resulting maximum peak pfd value is −126.05 dB(W/m^2 4 kHz).

FIGURE A3-1

pfd as a function of the elevation angle δ for the spaceborne VHF radar sounder (reference bandwidth of 4 kHz)

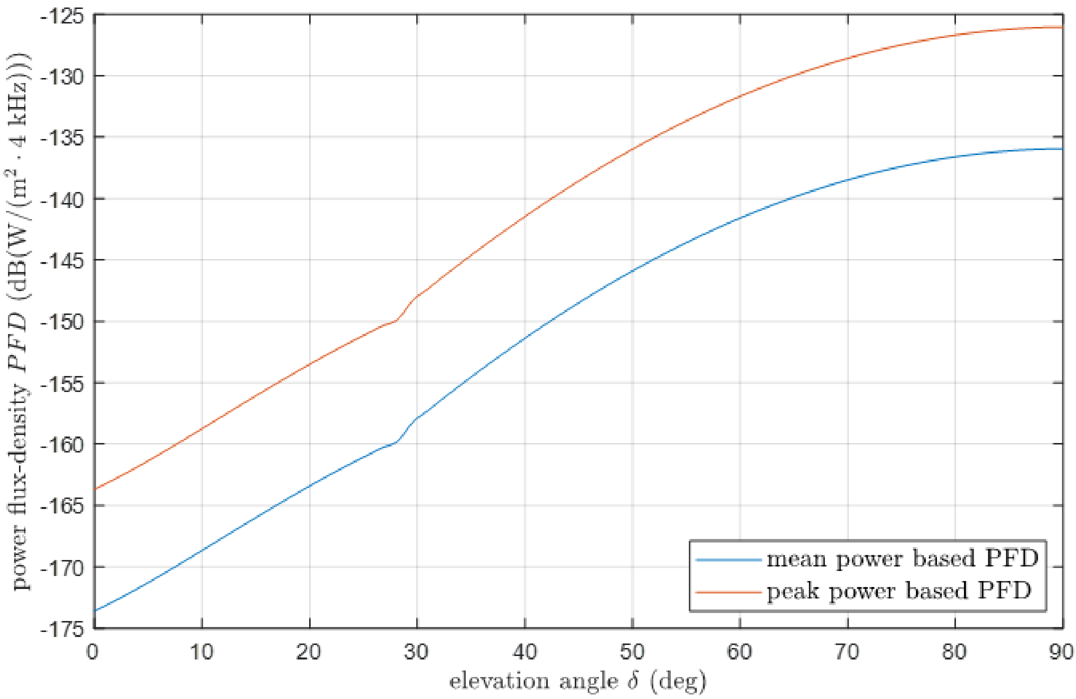

A3.2 Determination of relevant pfd levels for the protection of incumbent services – Generic approach

In order to help determine an appropriate limit to prevent harmful interference from occurring to a given incumbent service, it is beneficial to calculate the pfd that can protect the incumbent service.

$$PFD(\theta) = I - G_r(\theta) - 20\log(\lambda) + 10\log 10(4\pi) + L_p + \text{Feeder Losses} + 10\log10(4\text{ kHz}) \quad \text{(A3-4)}$$

where:

$$I = (I/N)_{\text{IPC}} + N \quad \text{(A3-5)}$$

Here, I is the maximum allowable interference PSD for the incumbent service under consideration (in dBW/Hz), while N is the overall noise PSD (also in dBW/Hz), given by equation (11) and calculated as in § 4.1.2. Based on the characteristics as summarised in Table A3-1, $G_r(\theta)$ was determined for each type of system using Recommendation ITU-R F.699.

TABLE A3-1

Receiving antenna gain values used to derive pfd levels for each system considered

Victim System	Frequency (MHz)	Gain (dBi)
FIXED	45	0
MOBILE	45	0

TABLE A3-1 *(end)*

Victim System	**Frequency (MHz)**	**Gain (dBi)**
BROADCASTING (DRM)	45	−0.05
BROADCASTING (TV)	45	0.15
Radiolocation	45	0
Radiolocation (WPR)	47	34
AMATEUR	45	2.5

The values given in Table A3-2, that represent the maximum pfd limits calculated at 0 degrees elevation angle can be used for protecting the incumbent services.

TABLE A3-2

Derivation of pfd limits from the protection criteria of incumbent services in 4 kHz

Victim system	**pfd limit (dBW / (m^2. 4 kHz))**
FIXED	−155
MOBILE (−6 dB *I*/*N* IPC)	−152
MOBILE (−10 dB *I*/*N* IPC)	−156
BROADCASTING (DRM)	−166
BROADCASTING (TV)	−166
Radiolocation	−155
Radiolocation (WPR)	−189
AMATEUR	−155

It should be highlighted that this generic method leads to pfd levels that are not compatible with EESS (active) operations. Indeed, it does not take into account the operational characteristics of the sensors and the highly varying nature of their potential interference to other services, as outlined in the studies described in the previous Annexes. An EESS (active) allocation associated with such pfd limit would hence not allow to design an EESS sensor that can meaningfully operate in the band.

A3.3 Determination of relevant pfd levels for the protection of incumbent services – Specific approach

In order to help determine an appropriate limit to prevent harmful interference from occurring to a given incumbent service, it is beneficial to calculate the pfd that can protect the incumbent service.

Considering the results of the studies provided in the previous sections, this section proposes to determine the required pfd levels for the protection of the incumbent services.

The methodology used to determine the pfd of the protection of the incumbent services is described below, taking the example of the protection of the mobile service:

1 Extract the maximum exceedance of the protection criteria of each service starting from the IEL exceedance studies (see Annex 2):

TABLE A3-3

Exceedance of protection criteria using the mean power (see Table A2-1)

Service	**Units**	**Exceedance of protection criteria**
MOBILE, $I/N = -6$ dB (rural)	dB	8.6

2 Consider the pfd of the spaceborne radar sounder as described in § A3.1:

TABLE A3-4

Mean pfd of the spaceborne radar sounder

Frequency	**Units**	**Mean pfd level (dB(W/(m^2 · 4 kHz)))**
45	MHz	−136

3 Remove from the pfd of the spaceborne radar sounder the exceedance of the protection criteria.

4 If the supplementary attenuation of the ionosphere was considered in the static studies from step 1, remove the attenuation of the ionosphere to obtain the required pfd level independently from the location of the victim receiver (for the mid-latitude location, the attenuation used in the calculations in Annex 2 was assumed to be 2.3 dB).

TABLE A3-5

pfd for the protection of the incumbent services

Frequency	**Units**	**pfd (dB(W/(m^2 · 4 kHz)))**
45	MHz	−146.9

In the procedure described above, mid-latitudes were considered. Recommendation ITU-R P.531 makes a distinction between mid-latitudes and polar locations for the evaluation of the ionospheric attenuation. This might be taken into account when assessing the allowable pfd level at a specific location for the victim receiver.

Annex 4

Sensitivity analysis – Considerations related to reduced operational duty cycle in polar regions

Recall from § 2.4 that the operational duty cycle, which represents the maximum percentage of time for which the spaceborne VHF radar sounder is active over a single spacecraft orbit, is approximately 10.79%, which is calculated with the designed total operational duration (10 minutes) and spaceborne VHF radar sounder orbit cycle (92.7 minutes). The operational duty cycle does not take into account the signal duty cycle.

In practice, data measurements from the sounder may not need to be taken at every orbit, but may be reduced according to the requirements of the mission and scaled according to the expected rate of change of the area to be imaged.

In comparison to previous sections that consider the 10.79% operational duty cycle which is applicable to a reference time period of a single orbit of 92.7 minutes, this Annex evaluates an example case where the transmissions are limited to 0.05% of the time over an 18 month reference time period.

However, considering any duty cycle value (e.g. between 0.05% and 10.79%) should be made at first in the light of its compatibility with EESS (active) operations. As an example, the impact to the incumbent service systems at the victim site at Alert, Nunavut, in Canada, when an operational duty cycle of 0.05% is in effect can considered. Recall from §§ A1.2, A1.3 and A1.4, that when the victim site was at Alert, the percentage of time over which the IEL exceeded the 0 dB threshold was approximately seven times higher than when the victim site was at Ghardaïa. This can be attributed to the fact that Alert is very close to the northern arc of the sounder orbit, and as such, is visible from the sounder at every orbit pass. This is in contrast with the victim site at Ghardaïa, nearer the Equator, which is only visible from the sounder when the orbit passes shift into view. To reduce the percentage of time over which the IEL exceeds the 0 dB threshold for harmful interference, an operational duty cycle of 0.05%, as opposed to the nominal value of 10.79%, was analysed.

Dynamic RFI simulations were carried out using Alert as a victim site, and with an operational duty cycle of 0.05% in force. In Table A4-1, some of the results from these dynamic RFI simulations can be found. Specifically, the maximum received peak interference power and IEL values, along with the percentage of time for which the peak power based IEL exceeded the 0 dB threshold, are given for a variety of victim scenarios. For this table, only a rural external noise environment was considered, as this represents the most stringent case, in terms of allowable interference. As can be seen, reducing the operational duty cycle from 10.79% to 0.05% dramatically reduced the percentage of time for which the IEL exceeded the 0 dB threshold for harmful interference.

TABLE A4-1

Maximum received peak interference power and IEL values, along with the IEL 0 dB exceedance percentage of time, for all incumbent service sharing study sets, assuming a victim site at Alert, Nunavut, a rural external noise environment, and transmission 0.05% of the time

Victim scenario description	Receiver antenna tilt angle (degrees)	Dynamic analysis maximum received peak interference power P_r (dBW)	Dynamic analysis maximum IEL (dB)	Percentage of time IEL exceeds 0 dB (%)
FIXED	5	−117.28	25.00	0.0042
FIXED	10	−115.67	26.61	0.0041
MOBILE (−6 dB *I*/*N* IPC)	0	−116.24	22.80	0.0038
MOBILE (−6 dB *I*/*N* IPC)	5	−114.90	24.14	0.0038
MOBILE (−10 dB *I*/*N* IPC)	0	−116.24	26.80	0.0050
MOBILE (−10 dB *I*/*N* IPC)	5	−114.90	28.14	0.0050
BROADCASTING (DRM)	5	−111.76	40.26	0.0054
BROADCASTING (DRM)	10	−110.15	41.87	0.0054
BROADCASTING (ST61 TV)	5	−100.70	32.12	0.0053
BROADCASTING (ST61 TV)	10	−99.09	33.72	0.0053
Radiolocation	0	−107.80	29.08	0.0052
Radiolocation	5	−106.47	30.41	0.0052
Oceanographic radar (System 4)	N/A	−152.06	8.42	0.0005
Oceanographic radar (System 9)	N/A	−144.31	11.64	0.0014
WPR (Rec. ITU-R M.1226)	N/A	−67.37	57.06	0.0043
WPR (Rec. ITU-R M.1851-1)	N/A	−63.77	60.66	0.0046
Space research	N/A	−139.07	18.77	0.0005
AMATEUR (Section 9 OoB analysis)	5	−148.69	−2.89	0
AMATEUR (Section 9 OoB analysis)	10	−147.08	−1.28	0
AMATEUR (Rec. ITU-R SM.1541-6 spectral mask)	5	−131.18	14.62	0.0009
AMATEUR (Rec. ITU-R SM.1541-6 spectral mask)	10	−129.58	16.23	0.0009